Integration of Design and Control under Uncertainty: A New Back-off Approach using PSE Approximations

by

Siddharth Mehta

A thesis

presented to the University of Waterloo

in fulfillment of the

thesis requirement for the degree of

Master of Applied Science

in

Chemical Engineering

Waterloo, Ontario, Canada, 2016

Author's Declaration

I hereby declare that I am the sole author of this thesis. This is a true copy of the thesis, including any required final revisions, as accepted by my examiners.

I understand that my thesis may be made electronically available to the public.

Abstract

Chemical process design is still an active area of research since it largely determines the optimal and safe operation of a new process under various conditions. The design process involves a series of steps that aims to identify the most economically attractive design typically using steady-state optimization. However, optimal steady-state designs may fail to comply with the process constraints when the system under analysis is subject to process disturbances (e.g. the composition of a reactant in a feed stream) or parameter uncertainty (e.g. the activation energy in a chemical reaction). Moreover, the practice of overdesigning a process to ensure feasibility under process disturbances and parameter uncertainty has been proven to be costly. Therefore, a new methodology for simultaneous design and control for dynamic systems under uncertainty has been proposed. The proposed methodology uses Power Series Expansions (PSE) to obtain analytical expressions for the process constrains and cost function. The key idea is to use the back off approach from the optimal steady state design to address the simultaneous process and design problem in an efficient systematic manner using PSE approximations. The challenge in this method is to determine the magnitude of the back-off needed to accommodate the transient and feasible operation of the process in presence of disturbances and parameter uncertainty. In this approach, PSE functions are used to obtain analytical expressions of the actual process constraints and are explicitly defined in terms of system's uncertain parameter and the largest variability in a constraint function due to time-varying changes in the disturbances. Also, the PSE approximation for each constraint is developed around a nominal point in the optimization variables and for each realization considered for the uncertain parameters. The PSE-based constraint represents the actual process constraint and can be evaluated faster since it is explicitly defined in the terms of the

optimization variables. The work focuses on calculating various optimal design and control parameters by solving various sets of optimization problems using mathematical expressions obtained from power series expansions. These approximations are used to determine the direction in the search of optimal design parameters and operating conditions required for an economically attractive, dynamically feasible process. The proposed methodology was tested on an isothermal storage tank and a step by step procedure to develop the methodology has been presented. The methodology was also tested on a non-isothermal CSTR and the results were compared with the formal integration process. Effect of tuning parameter, which is a key parameter in the methodology, have been studied and the results show that the quality of the results improves when smaller values of tuning parameter are used but at the expense of higher computational costs. The effect of the order of the PSE approximation used in the calculations has also been studied and it shows that the quality in the results is improved when higher orders in the PSE approximations are used at the expense of higher computational costs. The methodology was also tested on a large-scale Waste Water treatment plant. A comparison was made for different values of tuning parameters and the most feasible value was chosen for the case study. Effects of different disturbances profiles such as step and ramp changes were also studied. The studies concluded that a lower cost value is obtained when ramps are used as disturbance profile when compared with step changes. The methodology was also tested when parameter uncertainty was introduced and the results show a higher cost is required when uncertainty is present in the system when compared with no uncertainty.

The results show that this method has the potential to address the integration of design and control of dynamic systems under uncertainty at low computational costs.

Acknowledgements

First and foremost, I would like to express my sincere gratitude to my supervisor Professor Luis Ricardez-Sandoval for his great support and guidance during my entire Master's program. Apart from the great deal of technical knowledge I have acquired under his supervision, I have also learned skills like communication and how to keep myself motivated in challenging conditions.

Furthermore, I would like to extend my thanks to the readers of my thesis, Professor Hector Budman and Professor William A. Anderson

I would like to thank my group members Bhusan Patil, Sami Bahakim, Mina Rafiei, M. Hossein Sahraei, Zhenrong He and Robert Koller for their continued help and assistance throughout my research studies. I would like to thank my Chem Eng friends like Sudhanshu Soman, Ushnik Mukherjee, Sannan Toor, Muhammad Umar Farooq and Injila Khan for being so generous in sharing their vast knowledge. I would like to thank all my friends at Waterloo for making my time here a very enjoyable experience.

Finally, I would like express my deepest gratitude to my parents who have always been there for me.

Table of Contents

List of Figures

List of tables

Nomenclature

List of English symbols

c	Dissolved oxygen concentration
CC	Capital Cost
CSTR	Continious Stirred Tank Reactor
Cv	Valve coeffient in the storage tank
d(t)	Process Disturbances
E	Activation Energy
F_{in}	Inlet stream flow rate in the strorage tank
F_{out}	Outlet stream flow rate in the storage tank
fk	Turbine speed
g_0	Standard gravity
H	Height of the storage tank
h	Process constraint vector
J	Set of realization of Uncertain Parameters
K	Stem position of the valve
k_0	Pre exponential factor
k_c	Cellular specific activity
k_d	Biomass death rate
LHS	Latin hypercube sampling

M	cost associated with process constraints
MC	Monte carlo sampling
MIDO	Mixed integer dynamic optimization
MINLP	Mixed integer non linear optimization problem
MPC	Model predictive control
N_{iter}	Maximum number of iteration
OC	Opertaing cost
PCE	Polynomial Chaos Expansion
PDF	Probability Distribution function
PI	Proportional Integral Controllers
PSE	Power Series Expansion
q	Vector of end point constraints
q_i	Inlet flow rate in the classifier
q_F	Inlet flow rate in the reactor
q_p	Purge flow rate
q_2	Recycle flow rate
s	Substarte concentration
s_{ir}	Substate concentration in inlet stream
T_F	Inlet feed temprature in the reactor
u(t)	Manipulated variables
w_j	Weights
x	State of the system

x	Biomass substarte
x_{ir}	Biomass concentration in the inlet of thebioreactor
y	Output of the system
y(t)	Controlled variables

List of Greek symbols

η	Optimization variables
ζ	Uncertain (time-invariant) parameters
ω	Process design variables
ξ	Controller tuning parameters
Θ	Annualized Cost
∇i	i^{th} order gradient in the PSE approximation
Z(i)	i^{th} sensitivity term in the PSE approximation
δ	Tuning parameter
$\boldsymbol{\eta}^{l}$	Lower bound on the optimization variables
$\boldsymbol{\eta}^{u}$	Upper bound on the optimization variables
ρ	Input saturation limit
λs,j	Optimization variable in the PSE approach
μ	Specific growth rate

Chapter 1

Introduction

Chemical processes are dynamic and complex systems in nature and are subjected to process disturbances and process uncertainty. Chemical process design is an important task carried out in order to achieve the desired output and quality of the final products taking into account the safety, environmental, operational and physical constraints at minimum possible capital, operating and dynamic variability cost. The design process typically involves a series of steps that aims to identify the most economically attractive design using steady-state optimization. Although chemical processes have been traditionally designed using this approach, the designs obtained from those analyses may fail to comply with the process constraints when it is subjected to process disturbances and uncertainty in the system's parameters. The resulting instances of infeasibility or constraint violations due to the presence of uncertainties have adverse effects on the process economics and the quality of the product obtained. Therefore, the design obtained from steady-state calculations at the nominal operating conditions may no longer be 'optimal' or even dynamically feasible when process disturbances and parameter uncertainty are introduced in the system. Since uncertainties are inevitable and inherent in almost every process, the conventional approach used to address this problem is to add overdesign factors [1, 2, 3], e.g., increasing the volume of a storage tank will aim to accommodate the uncertainty in the system at the expense of increasing the capital costs for this process. Any violation in the process constraint increases the operating cost of the process significantly. However, the main limitation with this approach is that

there is no systematic method to assign overdesign factors and is typically done from process experience, using process heuristics or even arbitrarily at times. Moreover, this practice of overdesigning a process to ensure feasibility under uncertainty has been proven to be costly. Therefore, one key challenge in process design is to specify an economically optimal system that can be operated safely and is dynamically feasible under a wide range of process disturbances and parameter uncertainty. This has motivated the development of systematic methods that explicitly account for dynamics in the calculation of the optimal process design. The aim of these methods is to analyze the effect of the system dynamics and then adjust the design of the plant (equipment size and operating conditions) to accommodate those dynamics and maintain the operation of the plant within its feasible limits. The designs obtained from the above discussed approach are expected to specify the most economically attractive process which is dynamically feasible in the presence of process disturbances and parameter uncertainty. Various methods have been proposed in this area and each of the methods has its own benefits and limitations in terms of, conservatism of the designs, ease of implementation, computational efficiency and its applicability to large-scale nonlinear chemical processes. The development of computationally-efficient methods that can be applied to design chemical plants is still an active area of research.

It is the aim of this study to develop a new practical approach using Power series expansion (PSE) approximations to address the problem of integration of design and control for chemical processes under process disturbances and parameter uncertainty. The key idea in this approach is to back-off from the optimal steady state design, which is often found to be dynamically inoperable due to the effect of process disturbances, process dynamics and parameter uncertainty. The key challenge in this method is to determine in a systematic fashion the magnitude of the back-off needed to

accommodate the transient and feasible operation of the process in the presence of disturbances and parameter uncertainty. The work focuses on calculating various optimal design and control parameters by solving various sets of optimization problems using mathematical expressions obtained from power series expansions. These approximations are used to determine the direction in the search of optimal design parameters and operating conditions required for an economically attractive, dynamically feasible process. The key benefit of this methodology is the significant reduction in the computational costs associated with the formal optimization framework used for solving the integration of design and control for chemical processes under uncertainty. The above stated approach for integration of design and control problem will be tested on three different case studies – a) A mixing storage tank, b) A non –isothermal Continuous Stirred Tank Reactor (CSTR) and c) a waste water treatment plant. These case studies were chosen based on their complexity and the degree of non-linearity. Each of these case studies will be analyzed in detail to investigate the benefits and limitations of the proposed back-off approach.

1.1 Research objectives

Based on the above, the research carried out in this work aims to achieve the following objectives:

i. Develop a practical and efficient method for simultaneous design and control of chemical processes under process disturbances and parameter uncertainty using PSE. The work focuses on calculating the amount of back-off required from the steady state design, which might be infeasible due to process dynamics and parameter uncertainty, to obtain the optimal design parameters that will result in a dynamically feasible and economically attractive process.

ii. Implement the method developed in this work to address the optimal design under process disturbances and parameter uncertainty for a non isothermal CSTR , a mixing storage tank and a highly nonlinear waste water treatment plant. This contribution will demonstrate the applicability of the proposed approach for the above mentioned case studies and the results obtained will be compared to the results obtained from the formal integration technique.

iii. Evaluate the effect of various key tuning parameters presented in this methodology on the optimal design of the Non isothermal CSTR , its economics and the computational costs.

1.2 Outline of the thesis

This thesis is organized in five chapters as follows:

Chapter 2 presents the literature review on the key subjects such as the concept of the back-off employed in this work. The studies relevant to the different methods in the field of integration of design and control are reviewed. Previous studies carried out to address the idea of back-off in integration of design and control are also discussed in detail. Uncertainty sampling techniques and the basic idea of Power series Expansion (PSE) approximation are also discussed in this chapter.

Chapter 3 presents the novel approach proposed in this work to address the optimal design of chemical processes in the presence of process disturbances and parameter uncertainty using PSE approximations. The key principles and procedures required to implement the proposed methodology are explained in this chapter. A simple case study featuring an isothermal storage tank design is presented here to illustrate the implementation of this methodology.

Chapter 4 presents a case study which involves the optimal design of a CSTR under process dynamics and parameter uncertainty using the new PSE based methodology. This section explains in detail how each process constraint and the cost functions are represented using the corresponding PSE approximations. The results obtained with and without uncertainty in the system's parameters are dissued in detail. The results are also compared with the formal integration technique in order to compare the economic viability of the new proposed methodology. The effect of various key parameters used in the methodology have been also discussed in detail. In order to test the proposed methodology using a complex system, a waste water treatment plant was also designed using the proposed methodology, whose results are presented in this chapter.

Chapter 5 summarizes the key research outcomes of the present study and discusses the future research avenues that can be further explored in this emerging area.

Chapter 2

Literature Review

Although the idea in simultaneous design and control is straightforward, there are challenges as it often involves a trade-off between the optimal steady state design and the corresponding process dynamics. Therefore, a unified framework to address this problem is not currently available; instead, multiple methodologies have been presented to perform simultaneous design and control. The studies relevant to the different methods and approaches to the optimal process design under process disturbances and parameter uncertainty are reviewed in this chapter. Several studies carried out to address the idea of back off in the context of integration of design and control have also been discussed in detail in this chapter. Uncertainty sampling techniques and the basic idea of Power series Expansion (PSE) approximation are presented at the end of this chapter.

2.1 Integration of design and control

The field of process design under process disturbances and parameter uncertainty has gained wide interest due to the fact that the process dynamics may cause serious operational problems if not accounted for at the design stage. In addition, the presence of uncertainty or process disturbances is almost inherent in every process due to lack of knowledge or imprecise measurements, making it a general design issue and not just specific to certain processes.

The problem of integration of design and control under process disturbances and parameter uncertainty can be conceptually posed as follows:

Minimize	Expected Total Annualized Cost (Θ)	
Subject to	Process model, Process design and control equations, Process constraints, Design specifications	(2.1)

The aim is to minimize the total annualized cost (Θ) which can further be broken down into the process capital and operating costs. Since process disturbances and parameter uncertainty will be accounted for in this problem, the expected value of the total capital (CC) and operating (OC) costs becomes the objective function to be minimized. Process disturbances $\mathbf{d}(t)$ and parameter uncertainty $\boldsymbol{\zeta}$ will result in variability in the outputs ($\mathbf{y}$) and states ($\mathbf{x}$) of the system, and thus in the evaluations of the process feasibility constraints which may include safety, environmental or operational constraints. Problem (2.2) is the mathematical optimization model for problem (2.1). This problem aims to search for the process design variables ($\boldsymbol{\omega}$) and the controllers tuning parameter ($\boldsymbol{\xi}$) that remain feasible with respect to the process constraints ($\mathbf{h}$) under the given set of disturbance profile $\mathbf{d}(t)$ and under realizations of uncertainty set $\boldsymbol{\zeta}$. The present analysis assumes that a dynamic model describing the behavior of the process is available for simulations.

$$
\begin{aligned}
&\min_{\boldsymbol{\eta} = [\boldsymbol{\omega}, \boldsymbol{\xi}]} \quad E[\Theta(\mathbf{x}(t), \mathbf{u}(t), \mathbf{y}(t), \boldsymbol{\zeta}, \mathbf{d}(t), \boldsymbol{\xi}, \boldsymbol{\omega})] \\
&\text{s.t.} \\
&\mathbf{f}(\dot{\mathbf{x}}(t), \mathbf{x}(t), \mathbf{u}(t), \mathbf{y}(t), \boldsymbol{\zeta}, \mathbf{d}(t)\,, \boldsymbol{\omega}) = 0 \\
&\mathbf{g}(\dot{\mathbf{c}}(t), \mathbf{c}(t), \mathbf{u}(t), \mathbf{y}(t), \boldsymbol{\xi}, \mathbf{d}(t), \boldsymbol{\omega}) = 0 \\
&\mathbf{q}(\mathbf{x}(t), \mathbf{u}(t), \mathbf{y}(t), \mathbf{d}(t), \boldsymbol{\zeta}, \boldsymbol{\omega}, t_e) \leq 0 \\
&\mathbf{h}(\mathbf{x}(t), \mathbf{u}(t), \mathbf{y}(t), \mathbf{d}(t), \boldsymbol{\zeta}, \boldsymbol{\omega}) \leq 0 \\
&\boldsymbol{\eta}^{LB} \leq \boldsymbol{\eta} \leq \boldsymbol{\eta}^{UB}
\end{aligned}
\qquad (2.2)
$$

The decision variables ($\boldsymbol{\eta}$) comprise of the process design variables ($\boldsymbol{\omega}$) and the controller tuning parameters ($\boldsymbol{\xi}$). Moreover, $\mathbf{f}$ and $\mathbf{g}$ represents the set of differential and algebraic process model

and controller equations, respectively; **q** is the vector of end-point constraints evaluated at time t_e. The objective function is the expected value of the cost function (Θ) which is typically represented by the capital and operating costs.

Integration of design and control is an active area of research in chemical engineering and various different schemes have been presented in the literature. There is no unified framework available as of now because every methodology which have been developed have their own advantages and limitations. The prominent works in the field of integration of design and control area are disused next.

Perkins and Walsh [4] proposed the design under worst case scenarios during dynamics of the system and selection of optimal control schemes. Methods, based on optimization, to assess controllability and to develop integrated design of process and control system for cases where dynamic performance is critical were presented in that study. Luyben and Floudas [5] presented a systematic procedure to study the simultaneous design and control at the process synthesis stage by incorporating both steady-state economics and open loop controllability measures within a multi-objective mixed integer nonlinear optimization problem (MINLP). Alhammadi and Romagnoli [6] proposed a step-by-step integrated framework that incorporates economical, environmental, heat integration and controllability aspects of the process to be designed. Steady-state controllability indicators were used to measure the process dynamic performance.

Mohideen et al. [7] introduced the concept of simultaneous design and control in the presence of uncertain parameters while using formal mixed-integer dynamic optimization methods (MIDO). In that work, disturbances were allowed to follow a user-defined function with unknown (critical) parameters whereas the uncertain parameters' range of space was reduced to a set of discrete events or scenarios. A mixing tank problem and a ternary distillation design problem was used to

demonstrate the potential of the approach. The results obtained were then compared with the sequential approach. Bansal et.al [8, 9] improved the methodology proposed by Mohideen et al. by solving a formal dynamic optimization problem that aims to estimate the disturbance profile of the system that produces the worst-case scenario. Both continuous and discrete decisions were explicitly considered in the analysis. Kookos [10] proposed a systematic methodology for the deterministic optimization of batch processes under uncertainty based on Monte Carlo simulation in order to evaluate the objective function and the process constraints together with their analytical derivatives with respect to the optimization parameters. Seferlis and Grievink [11] proposed a number of techniques based on a non-linear sensitivity analysis of the static and dynamic plant controllability properties that facilitate the process design and control in a fully optimized and integrated fashion. Chawankul et al. [12] and Gerhard et al [13] approximated the dynamic behavior of the system using suitable model structures which led to efficient computation of the worst case scenario. Another set of methodologies have approximated the dynamic behavior of the system using suitable model structures which led to efficient computation of the worst case scenario [14, 15, 16]. Therefore, these methods reduced the computation burden imposed by dynamic optimization methods and can be used for optimal design of large-scale processes. However, those methods may result in conservative designs since they are based on the identification of the worst-case scenario, which may not occur often during the actual operation of the plant. Model-based strategies for simultaneous process and design have also been proposed. Sanchez-Sanchez and Ricardez-Sandoval [17, 18] integrated the dynamic feasibility and flexibility in a single stage optimization problem and robust stability test was performed in presence of magnitude bounded perturbations. The approach was tested using standard feedback controllers and Model Predictive controllers (MPC). Bahakim and Ricardez-Sandoval [19] proposed an

optimization framework with the aim of achieving a feasible and stable optimal process design in the presence of stochastic disturbances using Model Predictive Control (MPC). A case study of a waste water treatment plant was studied using the methodology proposed by those authors and compared it with the sequential design approach. Vega and Lamanna [20] proposed a multi-objective integration of design and control methodology and its successful application on an activated sludge process in a waste water treatment plant. Xia and Zhao [21] proposed a new methodology for steady state optimal design of chemical processes with robust stability constraints under parametric uncertainty and disturbances. Trainor et.al [22] incorporated robust flexibility, feasibility and stability analyses within a proposed simultaneous design and control methodology to ensure process dynamic operability and asymptotic stability in the presence of the worst-case scenario. Reviews on integration of design and control can be found elsewhere. [23, 24, 25, 26].

The present work focuses on a new methodology for simultaneous design and control using PSE approximations. The idea of this approach is to back-off from the optimal steady-state design point to a new operating condition which will be feasible under the given set of process dynamics and parameter uncertainty. Figure 2.1 illustrates the basic idea of back-off approach. Figure 2.1(a) shows that the optimal design point is feasible at steady-state conditions. However, this point might violate the constraints when transient changes are accounted for in the analysis as shown by red dotted circle in Figure 2.1(a). In order to accommodate process dynamics, the optimal steady state design has to be shifted (back-off) to a new feasible operating region. Figure 2.1(b) shows the direction and the magnitude of back-off that is required to specify a new feasible operating point under process disturbances and parameter uncertainty .The method proposed in this work will be explained in detail in the next chapter.

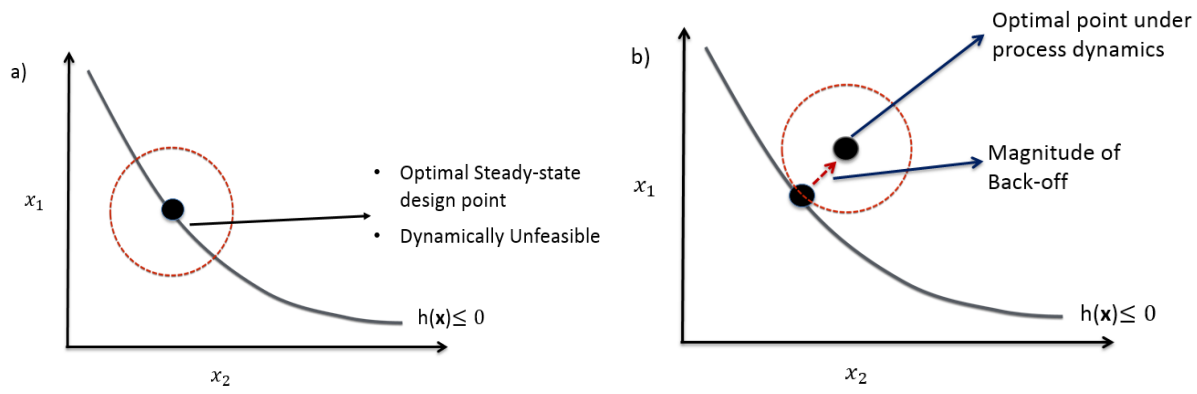

Figure 2.1 Idea of Back-off

The idea of back off in simultaneous design and control was initially proposed by Bahri et.al [27, 28]. In that work, the authors developed a method for determining the necessary open-loop back off from a steady state optimal point to ensure feasibility in presence of process disturbances. The approach consisted of defining a joint optimization-flexibility problem that can be solved in an iterative fashion at steady-state. The algorithm developed was based on a decomposition method which was broken into two levels of optimization problem. The first optimization problem seeks the optimality of steady state open loop problem with flexibility for a fixed set of disturbances. The second optimization problem evaluates the feasibility of the design found in the previous stage using different sets of disturbance profiles. Three examples were presented to illustrate the application of this approach: (1) a simple linear example, (2) a system of two CSTRs; and (3) an industrial distillation column. Figueroa et.al [29] extended the method proposed by Bahri to consider process dynamics, i.e. they proposed a joint dynamic optimization flexibility analysis for integration of design and control. In that approach, the optimization of the controllers tuning parameters was also included. A model consisting of a series of CSTR's was used as an illustrative example to explain the methodology. Kookos and Perkins [30, 31] also used the idea of back-off for simultaneous process and control design problem. The idea was to analyze a sequence of

combined configurations making use of bounding schemes to successively reduce the size of the search region. A decomposition algorithm for solving the combined process and control design problem was used. The main idea in that work was to progressively generate tighter upper and lower bounds on the optimal dynamically feasible solution. Lower bounds were calculated by solving the improved steady state problem and the topology was optimized. Upper bounds were generated by solving the dynamic optimization problem keeping the topology fixed and the design parameters optimized. Case studies featuring an evaporator system, a binary distillation column, a reactor- separator with recycle process were used to test that methodology.

Most of the optimization-based methods available in literature for simultaneous design and control follow the same key concept; that is, determine (or specify) the critical realizations in the process disturbances and the process uncertain parameter that produce the largest deviations in the controlled variables. This condition is often termed as the *worst-case scenario,* and the variability created in the system due to this scenario is called the *worst-case process variability*. The worst-case scenario has been used by some of the simultaneous design and control methodologies to evaluate the process economics and the process constraints considered in the analysis. An optimal design and control scheme is referred to as the configuration that can accommodate the worst-case scenario (or critical scenarios identified *a priori*) in a safe and acceptable fashion without violating constraints in the control action movements or in the critical operating variables of the system. The challenge and difference in the approaches available in literature is in the method used to compute this worst-case scenario, e.g., using open-loop controllability indexes [3,9,10] from a formal dynamic optimization formulation [32], or from the implementation of robust control tools [18, 33].

One of the key challenges faced is the computational costs associated with the repetitive evaluation of the process constraints and cost function for every set of decision variables' values tested by the optimization algorithm. While this task may be relatively inexpensive for chemical processes described with just a few set of differential equations, the computational costs associated with this task while performing the integration of large-scale chemical systems is a daunting task that can become computationally prohibitive. The methodology developed in this thesis aims at reducing the computational costs by solving a set of simple optimization problems in an iterative manner.

2.2 Uncertainty quantification methods

Various uncertainty sampling methods have been proposed in the literature for uncertainty quantification. The Monte-Carlo (MC) sampling technique is one of the most popular methods used for sampling, which generates pseudorandom numbers to approximate a standard probability distribution function (PDF). Then, to obtain the specific values for each random variable, the pseudorandom samples are inverted over the cumulative distribution of the specified PDF for that variable. Another sampling technique called the Latin hypercube sampling (LHS) uses stratification sampling, which may provide more accurate estimates of the distribution function [34]. The range of the uncertain variables is divided into intervals of equal probability and a single value is sampled from each interval. In the case of multidimensional uncertainty, the pseudorandom samples obtained for one stochastic variable is randomly paired with all the other randomly sampled pseudorandom values of the other random variables. Florian [35] has proposed an efficient sampling scheme through an improved variant of the LHS which was called the Updated Latin Hypercube sampling, which results in a substantial decrease of the variance in the estimates of statistical parameters. Antithetic Variates (AV) method [36], is also one of the

sampling techniques that has been shown to reduce the mean squared error (bias) of an estimated statistical function when compared to the use of independent random sampling (such as MC); however, this is not as efficient as the Latin Hypercube Sampling technique [37]. Johnson et al [38] proposed a sampling method based on Maxmin designs, which spreads the sampling region around the entire domain space by maximizing the minimum distance between any two samples. The propagation of uncertainties via traditional Monte Carlo methods based on standard or Latin Hypercube sampling is valid for a wide range of problems; however, it is computationally expensive since it requires a large number of simulations .Efficient sampling methods nowadays make use of low-discrepancy sequences instead of random sampling as is the case with the Monte Carlo and Latin hypercube techniques. These methods, typically referred to as quasi-Monte Carlo methods, usually converge faster than techniques employing random or pseudorandom sequences. Since the Monte Carlo sampling and the Latin hypercube sampling methods are computationally expensive, other methods have to be developed which are more efficient than these sampling techniques. Polynomial chaos Expansion (PCE), is also a non-sampling-based method to determine evolution of uncertainty in dynamic system, when there is probabilistic uncertainty in the system parameters. Wiener's polynomial chaos is fundamentally a framework for separating stochastic components of a system response from deterministic components. It is derived from the Cameron–Martin theorem which establishes that a random process with finite second-order moments can be decomposed into an infinite, convergent series of polynomials in a random variable. The key idea for using PCE's is that the variance of the predicted outputs can be rapidly calculated by an analytical expression thus critically reducing computational times [39, 40]. The polynomial chaos expansion can be used for studying the uncertainty propagation in open-loop or closed-loop systems, and can be applied for uncertainties in model parameters, initial conditions,

or inputs of the systems. Hence, the polynomial chaos is an efficient alternative to Monte Carlo simulations for complex systems.

In this thesis, Power Series Expansion (PSE) approximations has been used extensively; hence, this uncertainty quantification method will be revised in detail next.

2.2.1 Power Series Expansion Method

Since the Monte Carlo sampling and the Latin hypercube sampling methods are computationally expensive, other efficient methods are needed to assess uncertainty quantification. One way to address this issue is to use the sensitivity analysis technique. This method represents the prediction as a perturbation around its nominal value, which is associated with the mean or expected value of the uncertain deterministic problem. Sensitivity analysis usually provides reliable predictions only when the associated perturbations are small, and cannot used to predict the shape of the whole distribution [40]. Like the PCE, PSE can be used for studying the uncertainty propagation in open-loop or closed-loop systems, and can be applied for uncertainties in model parameters, initial conditions, or inputs of the systems. First, second or even higher order power series expansions can be considered for the sensitivity analysis. The first-order method can be computationally efficient way to propagate uncertainties but for highly nonlinear processes the order of the power series expansion may have to be increased in an attempt to obtain an optimal solution, which in turn will require higher computational costs. PSE has been used in this work for the calculation of the sensitivities. Using Power Series Expansions, complex, nonlinear functions can be replaced by a polynomial function with a finite number of terms.

Assume f(x) is a complex function. Then, using power series expansion (PSE) approximation, f(x) can be represented as follows:

$$f(x) = f(x_{nom}) + \mathbf{Z}^{(1)}(x - x_{nom}) + \frac{1}{2}(x - x_{nom})^T \mathbf{Z}^{(2)}(x - x_{nom}) \ldots \quad (2.1)$$

Where,

$\mathbf{Z}^{(1)} = \frac{\partial f}{\partial x}$

$\mathbf{Z}^{(2)} = \frac{\partial^2 f}{\partial x^2}$

This equation can be generalized as follows:

$$f(x) = f(x_{nom}) + \sum_{n=0}^{\infty} \frac{f^{(n)}(x)}{n!} (x - x_{nom})^n \quad (2.2)$$

$\mathbf{Z}^{(1)}$ and $\mathbf{Z}^{(2)}$ are the first order and second order sensitivity terms. Generally, sensitivity analysis calculates the rates of change in the output variables in the system which results from perturbations in the systems various parameters. It should be noted that the above stated expansion is only valid around x_{nom}. Using this method, while designing any chemical process, nonlinear process design equations, nonlinear process constraints and the cost function can be represented in this form. It should be noted that higher order approximation will lead to more accurate approximations at the expense of higher computational costs. Higher the order of approximation, the higher the computational costs. Note that the sensitivities can be calculated analytically or numerically. A few works presented in the literature have used PSE approximation for uncertainty propagation. Bahakim et. al [41] proposed an methodology for the optimal design under uncertainty where PSE approximations were used to approximate the process constraint and the cost function. The PSE functions were used to identify the variability in the process constraint functions and model outputs due to multiple realizations in the uncertain parameters. A ranking based approach was adopted where the user can set the probabilities for different process constraints. This methodology was tested on a heat exchanger system, the Tennessee Eastman process, and a post-combustion CO_2 capture pilot-scale plant [42]. Rasoulian and Ricardez- Sandoval [43, 44, 45, 46] proposed a model for multiscale modelling of material growth subjected to model parameter uncertainty that can

significantly affect the control and optimization objective of the process. In that method, PSE was employed to analyze the model uncertainty propagation. The results showed that the PSE based approach for uncertainty analysis was more computationally attractive as compared with the traditional Monte Carlo approach.

Summary

A review on the simultaneous design and control strategies that have been proposed in the literature is discussed in this chapter. The chapter also discussed the idea of back-off from the steady state design which had been used in the methodology presented in this work. Several studies carried out to address the idea of back off have been discussed in detail. The aim of the methodology presented is to obtain optimal design and control parameter under process dynamics by using PSE function to at low computational costs. Hence, various uncertainty sampling techniques have been discussed. Given it relevance to this work, PSE based uncertainty propagation has been explained in detail. The next chapter discusses the step by step procedure of developing the PSE based algorithm for integration and design and control.

Chapter 3

Optimal design of large-scale chemical processes under uncertainty: PSE -based approach

When process dynamics and parameter uncertainty are considered in a chemical system, the design obtained from a steady-state analysis might not be valid. In order to obtain a dynamically feasible design, it is required to move away or back-off from the optimal steady state design. Also, the process design equations and process constraints equations for a chemical process or in a large scale industry are highly complex and nonlinear in nature. Hence, high computational costs are often required to perform the optimal design. In order to reduce the computational demands while searching for the optimal design, approximations that can represent the key characteristics of the actual nonlinear system are required. Therefore, a novel approach has been developed in the area of integration of design and control where Power series expansions (PSE) are used to represent the complex and nonlinear equations.

The proposed methodology uses PSE to obtain analytical expressions for the process constrains and cost function. The key idea is to apply the back off approach from the optimal steady state design to address the simultaneous process and design problem in an efficient systematic manner using PSE approximations. A set of optimization problems is solved in an iterative manner, which is mathematically formulated using PSE approximations.

This chapter is structured in the sections as follows: Section 3.1 describes the disturbance profiles and uncertain parameters used in this methodology. Section 3.2 shows how each process constraint and the cost function is approximated using PSE approximations. The optimization frame work used in this methodology is presented in Section 3.3. The step-by-step procedure used in the

methodology is also shown in this section. Section 3.4 is the remarks section where the benefits and limitations of the methodology have been discussed. Section 3.5 gives an illustrative example how an isothermal storage tank has been designed using the methodology and the results have been discussed in detail. Note that the content of this chapter has been published in the Industrial & Engineering Chemistry Research Journal [47].

3.1 Disturbances and parameter uncertainty

The proposed back-off methodology assumes that the disturbances' dynamics **d**(*t*) follow time dependent profiles specified a *priori*, e.g. a series of step changes or a sinusoidal function. Other methodologies have also used the same approach to specify the disturbance dynamics with critical model parameters. Parameter uncertainty ($\boldsymbol{\zeta}$) is introduced in the system when an exact value of a particular parameter is considered to be unknown. In this methodology, the uncertain parameters' range of space is discretized to a finite set of realizations (J) that are also weighted based on their probability of occurrence, i.e. w_j. As it is explained in the next section, PSE based functions are developed for each specific realizations in the uncertain parameters ($\boldsymbol{\zeta}_j$).

3.2 PSE approximations

The process constraints **h** specify the feasible operating region for a process and is often described as a function of the manipulated variables **u**(t), the controlled variables **y**(t), the disturbances affecting the process **d**(t), and the realizations in the uncertain parameters $\boldsymbol{\zeta}$. In this approach, PSE functions are used to obtain analytical expressions of the actual process constraints and are explicitly defined in terms of system's uncertain parameter and the largest variability in a constraint function *h* due to time-varying changes in the disturbances. Also, the PSE approximation

for each constraint is developed around a nominal point in the optimization variables $\boldsymbol{\eta}_{nom}$ and for each realization considered for the uncertain parameters $\boldsymbol{\zeta}_j$. Accordingly, each nonlinear process constraint can be represented as a PSE-based constraint function:

$$h(\boldsymbol{\omega}, \mathbf{u}, \mathbf{y}, \boldsymbol{d}, \boldsymbol{\zeta}_j, t) \leq \rho \;\; \leftrightarrow \;\; h_{PSE}(t)|_{\boldsymbol{d}(t),\zeta_j} \leq \rho \tag{3.1}$$

where ρ represents the input (saturation) limit on the constraint; the PSE-based constraint function is defined as follows:

$$h_{PSE}(\boldsymbol{\eta})|_{\mathbf{d}(t),\boldsymbol{\zeta}_j} = h(\boldsymbol{\eta}_{nom}) + \nabla \boldsymbol{h}_j(\boldsymbol{\eta})(\boldsymbol{\eta} - \boldsymbol{\eta}_{nom}) + \tfrac{1}{2}(\boldsymbol{\eta} - \boldsymbol{\eta}_{nom})^T \nabla^2 \boldsymbol{h}_j(\boldsymbol{\eta})(\boldsymbol{\eta} - \boldsymbol{\eta}_{nom}) + \cdots \tag{3.2}$$

where, $\boldsymbol{\eta} \in R^{P\times 1}$ and $\boldsymbol{\eta}_{nom} \in R^{P\times 1}$; similarly,

$\nabla \boldsymbol{h}_j(\boldsymbol{\eta}) = [Z_{1,j}^{(1)}, Z_{2,j}^{(1)}, Z_{3,j}^{(1)}, \ldots Z_{p,j}^{(1)}, \ldots Z_{P,j}^{(1)}]$

$$\nabla^2 \boldsymbol{h}_j(\boldsymbol{\eta}) = \begin{bmatrix} Z_{11,j}^{(2)} & Z_{12,j}^{(2)} & \cdots & \cdots & \cdots & Z_{1P,j}^{(2)} \\ Z_{21,j}^{(2)} & Z_{22,j}^{(2)} & \cdots & \cdots & \cdots & Z_{2P,j}^{(2)} \\ \vdots & \vdots & & Z_{pl,j}^{(2)} & & \vdots \\ Z_{P1,j}^{(2)} & Z_{P2,j}^{(2)} & \cdots & \cdots & \cdots & Z_{PP,j}^{(2)} \end{bmatrix}$$

$$Z_{p,j}^{(1)} = \left.\frac{\partial h}{\partial \boldsymbol{\eta}_p}\right|_{\boldsymbol{\eta}=\boldsymbol{\eta}_{nom},\mathbf{d}(t),\boldsymbol{\zeta}_j} \tag{3.3}$$

$$Z_{pl,j}^{(2)} = \left.\frac{\partial^2 h}{\partial \boldsymbol{\eta}_p \partial \boldsymbol{\eta}_l}\right|_{\boldsymbol{\eta}=\boldsymbol{\eta}_{nom},\mathbf{d}(t),\boldsymbol{\zeta}_j}$$

where $\nabla \boldsymbol{h}_j(\boldsymbol{\eta})$ and $\nabla^2 \boldsymbol{h}_j(\boldsymbol{\eta})$ represent the first order and second order gradients, respectively.

In this work, $\nabla^i \boldsymbol{h}_j(\boldsymbol{\eta})$ represents the i^{th} order gradient of the optimization variables $\boldsymbol{\eta}$ with respect to worst-case (largest) variability observed in the time domain for the constraint function h due to the time-dependent realizations in the disturbances $\mathbf{d}(t)$ and the j^{th} realization in the uncertain parameter $\boldsymbol{\zeta}_j$. Figure 3.1 illustrates the idea to calculate the worst case variability point in constraint

h, around which $h_{PSE}(\boldsymbol{\eta})|_{\mathbf{d}(t),\zeta_j}$ is developed under process disturbances $\mathbf{d}(t)$ and the uncertain parameter.

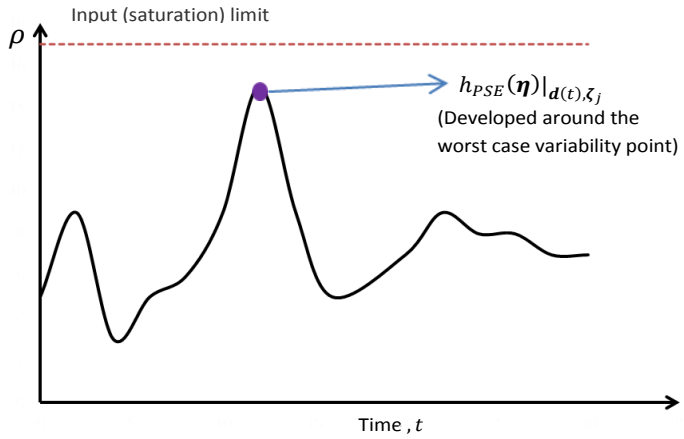

Figure 3.1: Worst case variability point around which PSE based functions are developed

The PSE-based constraint (h_{PSE}), represents the actual process constraint h and can be evaluated faster since it is explicitly defined in the terms of the optimization variables $\boldsymbol{\eta}$. Note that the h_{PSE} function shown in (3.2) can also be expanded to consider higher order terms, which will lead to accurate results at the expense of higher computational costs. Therefore, the choice of expansion order depends on the number of optimization variables $\boldsymbol{\eta}$, the system's degree of nonlinearity, the desired accuracy in the results, and the method used for calculating the sensitivity terms. In the present work, the finite difference method was employed to compute the sensitivity terms in the expansion, e.g. $Z_{p,j}^{(1)}$, $Z_{pl,j}^{(2)}$ as shown in (3.2). This method is the most commonly used to calculate sensitivities. Note that the computation of the sensitivity terms**,** involves a time-dependent term, i.e. the process disturbances **d**(t). The procedure to estimate $Z_{p,j}^{(1)}$, $Z_{pl,j}^{(2)}$ is as follows: The dynamic process model **f** and the controller equations **g** are simulated around a nominal point given by

$\boldsymbol{\eta}_{nom}$, and for the j^{th} realization in the uncertain parameters $\boldsymbol{\zeta}_j$. The inputs to these dynamic simulations are the time-dependent disturbances$\mathbf{d}(t)$, whose trajectory profiles remain fixed during the calculations. The simulation results are then used to identify the worst case deviation in time for the constraint function h (h^*) due to the realizations in $\mathbf{d}(t)$ and $\boldsymbol{\zeta}_j$, i.e.

$$h^*|_{\boldsymbol{\eta}_{nom,j}}=\max h(t)|_{\boldsymbol{\eta}_{nom},\mathbf{d}(t),\boldsymbol{\zeta}_j} \tag{3.4}$$

This procedure is then repeated for forward and backward values assigned to each optimization variable included in $\boldsymbol{\eta}$ while keeping the rest of the optimization variables constant at equal to their nominal values, i.e. $\boldsymbol{\eta}_{nom}$. For example, the largest (worst-case) deviation in a process constrain h due to a single realization in the uncertain parameters at the forward step for the p^{th} optimization variable can be expressed as follows:

$$h^*|_{\eta_{p,j}^+}=\max h(t)|_{\eta_p^+,\mathbf{d}(t),\boldsymbol{\zeta}_j} \tag{3.5}$$

Note that the rest of the decision variables included in $\boldsymbol{\eta}$ remain fixed and equal to their nominal values defined by $\boldsymbol{\eta}_{nom}$. Next, sensitivity terms, e.g. $Z_{p,j}^{(1)}$ and $Z_{pl,j}^{(2)}$, can be calculated using the data collected from the simulations. The first-order sensitivity term for the p^{th} decision variable at the j^{th} realization in the uncertain parameters can be calculated as follows:

$$Z_{p,j}^{(1)} = \left(h^*|_{\eta_{p,j}^+} - h^*|_{\eta_{p,j}^-}\right)/2\Delta\eta_p \tag{3.6}$$

where $\Delta\eta_p$ represents the difference between the forward step ($\eta_{p,j}^+$) and the backward step ($\eta_{p,j}^-$) for the p^{th} decision variable for the j^{th} realization in uncertain parameter. Similarly, the second order sensitivity term can be calculated as follows:

$$Z_{pp,j}^{(2)} = \left(h^*|_{\eta_{p,j}^+} - 2h^*|_{\boldsymbol{\eta}nom} + h^*|_{\eta_{p,j}^-}\right)/\Delta{\eta_p}^2 \tag{3.7}$$

Note that the first order and second order sensitivity terms are only valid around the nominal point $\boldsymbol{\eta}_{nom}$ and have been calculated using centered finite difference. Higher order sensitivity terms can be calculated using the same approach; however, additional forward and backward points around the nominal point are required. This same procedure can be used to formulate a mathematical expression for the cost function using PSE approximations, i.e.

$$\Theta_{PSE}(\boldsymbol{\eta})|_{\mathbf{d}(t),\boldsymbol{\zeta}_j} = \Theta(\boldsymbol{\eta}_{nom}) + \nabla\Theta_j(\boldsymbol{\eta} - \boldsymbol{\eta}_{nom}) + \frac{1}{2}(\boldsymbol{\eta} - \boldsymbol{\eta}_{nom})^T\nabla^2\Theta_j\,(\boldsymbol{\eta} - \boldsymbol{\eta}_{nom}) + \cdots \tag{3.8}$$

where, $\nabla\Theta_j$and $\nabla^2\Theta_j$are the first order and second order gradients for the cost function at the j^{th} realization in uncertain parameter $\boldsymbol{\zeta}$ and that are evaluated around the nominal point $\boldsymbol{\eta}_{nom}$ under process disturbances $\mathbf{d}(t)$ and for each realization in the uncertain parameters $\boldsymbol{\zeta}_j$.

3.3 Optimization problem and algorithm

Based on the above definitions, a PSE-based optimization problem can be formulated as follows:

$$\underset{\boldsymbol{\eta},\boldsymbol{\lambda}}{min} \quad \sum_{j=1}^{J} w_j\,\Theta_{PSE}(\boldsymbol{\eta},\mathbf{d}(t),\boldsymbol{\zeta}) + \sum_{j=1}^{J}\sum_{s=1}^{S} M\,\lambda_{s,j}$$

Subject to:

$$\begin{aligned}
&h_{PSE}^{s,max}\left(\boldsymbol{\eta},\mathbf{d}(t),\boldsymbol{\zeta}_j\right) - \rho\,(1+\lambda_{s,j}) \le 0 \qquad \forall s = 1,\dots,S;\ \forall j = 1,\dots,J\\
&h_{PSE}^{s,min}\left(\boldsymbol{\eta},\mathbf{d}(t),\boldsymbol{\zeta}_j\right) + \rho\,(1-\lambda_{s,j}) \le 0 \qquad \forall s = 1,\dots,S;\ \forall j = 1,\dots,J\\
&\boldsymbol{\eta}_{nom}(1-\delta) \le \boldsymbol{\eta} \le \boldsymbol{\eta}_{nom}(1+\delta).\\
&\sum_{j=1}^{J} w_j = 1\\
&\lambda_{s,j} \ge 0
\end{aligned} \tag{3.9}$$

where δ is a tuning parameter that determines the lower and upper bounds on the optimization variables ($\boldsymbol{\eta}$) . That is, this parameter determines the size of the search space region in the optimization variables that will be considered while solving problem (3.9). Moreover, $w_j$is a weight assigned to the probability of occurrence of the j^{th} realization in the uncertain parameters.

The decision variables $\boldsymbol{\eta}$ includes the process design variables ($\boldsymbol{\omega}$) and the controller tuning parameters ($\boldsymbol{\xi}$), i.e. $\boldsymbol{\eta} = [\boldsymbol{\omega}, \boldsymbol{\xi}]$. The first PSE-based constraint equation shown in (3.9) is employed when the worst case variability is calculated in the positive (maximum) direction whereas the second PSE-based constraint is used when the worst case variability is calculated in the negative (minimum) direction. Since all the constraints and the cost function are represented using PSE functions, the above optimization problem can be efficiently solved using standard optimization subroutines.

As mentioned above, the present approach aims to perform the back-off from the optimal steady-state design point. Therefore, active constraints identified from the optimal steady-state design problem are expected to be violated when process dynamics are first considered in the analysis. Accordingly, problem (3.9) may become infeasible when $\boldsymbol{\eta}_{nom}$ is set to be the point obtained from the optimal steady-state design or a nearby operating point. To avoid potential infeasibilities, an additional term has been added to the PSE-based cost function shown in problem (3.9). This term represents a penalty cost and is used to penalize any constraint violations that may occur while searching for the optimal design parameters that minimize the PSE-based cost function shown in problem (3.9). $\lambda_{s,j} \in \boldsymbol{\lambda}$ is an optimization variable and represents the magnitude in the s^{th} constraint function $\mathbf{h}_{PSE}^{s}$ that is required to be added (removed) to avoid infeasibility. *M* represents a big number that needs to be degrees of magnitude higher than the actual cost function. Note that there is one $\lambda_{s,j}$ for each constraint function h_{PSE}^{s} and each realization in uncertain parameter $\boldsymbol{\zeta}_j$. Alternatively, if the solution from (3.9) returns $\lambda_{s,j} \neq 0$, then the solution obtained for $\boldsymbol{\eta}$ determines a search direction for the process design and control variables, i.e. $\boldsymbol{\omega}$ and $\boldsymbol{\xi}$. Note that the design and control parameters obtained from problem (3.9) are valid around a region near by $\boldsymbol{\eta}_{nom}$, i.e., h_{PSE} and $\Theta_{PSE}$are developed around that nominal point; accordingly, the search space

for $\boldsymbol{\eta}$ in (3.8) is determined based on $\boldsymbol{\eta}_{nom}$ and the tuning parameter δ, which determines the magnitude of the feasible search space. Problem (3.9) represents the core calculation in the present back-off algorithm; this optimization problem works in an iterative manner as the result obtained from one iteration is used as the nominal (starting) point for the next iteration. Accordingly, the procedure proposed for the present back-off methodology is as follows:

Step 1: *Initialization*

The approach is initialised by defining the trajectory profiles for the disturbances $\mathbf{d}(t)$; the set of realizations for the uncertain process parameters $\boldsymbol{\zeta}$; initial guesses for the control tuning parameters ($\boldsymbol{\xi}$) and the process design variables ($\boldsymbol{\omega}$). Also, set the tuning parameter δ, the order of the PSE approximation to be used in the calculations, the maximum number of iterations (N_{iter}), a tolerance criterion for convergence (ε), and M. Further, the iteration index i is set to i=0.

Step 2: *Optimal steady-state design under uncertainty*

Perform the optimal steady-state design under uncertainty, i.e.

$$
\begin{aligned}
&\min_{\boldsymbol{\eta}} \quad \textstyle\sum_{j=1}^{J} w_j\, \Theta_{SS}\left(\boldsymbol{\eta}, \mathbf{d}, \boldsymbol{\zeta}_j\right) \\
&\mathbf{f}\left(\boldsymbol{\omega}, \mathbf{u}, \mathbf{y}, \mathbf{d}, \boldsymbol{\zeta}_j\right) = \mathbf{0} \qquad \forall\, \mathrm{j} = 1, \qquad (3.10)\\
&\mathbf{h}\left(\boldsymbol{\omega}, \mathbf{u}, \mathbf{y}, \mathbf{d}, \boldsymbol{\zeta}_j\right) \leq \mathbf{0} \qquad \forall\, \mathrm{j} = 1, \ldots, \mathrm{J} \\
&\mathbf{d} = \{\mathbf{d}^l, \mathbf{d}^u\}
\end{aligned}
$$

As shown in (3.10), the disturbances are treated as uncertain time-invariant parameters with discrete realizations given by their corresponding set of upper and lower bounds. The formulation presented in (3.10) corresponds to the optimal design of a system using discrete realizations j in the uncertain parameters; hence, the multi-scenario approach has been used to solve this optimization problem. Note that in the optimal steady state design formulation $\boldsymbol{\eta} = \boldsymbol{\omega}$ .The

solution obtained from this problem ($\boldsymbol{\eta}^0$) represents the most economical steady-state design that can be accomplished under parameter uncertainty; therefore, $\boldsymbol{\eta}^0$ is used as the initial point to start the present back-off methodology, i.e. $\boldsymbol{\eta}^0 = \boldsymbol{\omega}^0$.

At any iteration step *i*:

Step 3: *Develop the PSE-based functions*

Using $\boldsymbol{\eta}^0$ ($\boldsymbol{\eta}^i$) as the nominal operating point for the first (i^{th}) iteration, PSE-based functions are developed for each constraint *h* (i.e.h_{PSE}) considered in the formulation and also for the cost function (i.e. Θ_{PSE}). The expressions for h_{PSE} and $\Theta_{PSE}$are shown in (3.2) and (3.8), respectively.

Step 4: *Optimization of the PSE-based functions*

Formulate the PSE-based optimization problem (3.9) using the PSE functions developed in Step 3, the tuning parameter δ, and the current nominal point $\boldsymbol{\eta}^i$. The solution to this problem ($\boldsymbol{\eta}^{i+1}$) represents an improvement in the search direction for the optimal design variable ($\boldsymbol{\omega}^{i+1}$) and controller tuning parameters ($\boldsymbol{\xi}^{i+1}$), i.e. $\boldsymbol{\eta}^{i+1}$**= [**$\boldsymbol{\omega}^{i+1}$**,** $\boldsymbol{\xi}^{i+1}$**].**

Step 5: *Convergence criterion*

As shown in (3.11), a floating average convergence technique is used as a stopping criterion in this work. In this method, a sampling period *N* is specified first; then the mean of the PSE-based cost function obtained from iterations *i-2N+1* to *i-N* are subtracted from the mean of the same function obtained from iterations *iter-N+1* to *i*; if the difference in means, i.e. the costs, is less than a threshold value (ε), then the approach has converged.

$$Tol_{float}^{\Theta} = \frac{1}{N}\left(\sum_{m=i-2N+1}^{i-N}\Theta_m - \sum_{n=i-N+1}^{i}\Theta_n\right) \qquad (3.11)$$

where Θ_m and Θ_n represent Θ_{PSE} obtained from the solution of problem (3.11) at the m^{th} and n^{th} iteration as shown in (10), respectively. Similarly, for the optimization variables:

$$Tol_{float}^{\eta} = \frac{1}{N}\left(\sum_{m=i-2N+1}^{i-N} \eta_m - \sum_{n=i-N+1}^{i} \eta_n\right) \quad (3.12)$$

where η_m and η_n represent the value obtained from the solution of problem (3.9) for the optimization variable η at the m^{th} and n^{th} iterations as shown in (3.12), respectively. Accordingly, norms on the vector $\boldsymbol{Tol}_{float}^{\eta}$, i.e. $\left|\boldsymbol{Tol}_{float}^{\eta}\right|_p$, can be computed to determine the convergence in the optimization variables; typically the Euclidean norm ($p = 2$) or the infinity norm ($p = \infty$) can used to test for convergence. This same approach is employed to check for the convergence of the algorithm on each $\lambda_{s,j}$, i.e. $\left|\boldsymbol{Tol}_{float}^{\lambda}\right|_p$. If $\left|\mathbf{Tol}_{\text{float}}^{\lambda}\right|_{\text{p}}$ is below the threshold value (ε), and either $\text{Tol}_{\text{float}}^{\Theta}$ or $\left|\mathbf{Tol}_{\text{float}}^{\eta}\right|_{\text{p}}$ are below a threshold value (ε), then STOP, an optimal solution has been found, *i.e.* $\boldsymbol{\eta}^{i+1}$. Otherwise, set *i=i+1* and go back to Step 3. Alternatively, the algorithm is also terminated if the maximum number of iterations is reached, i.e. $i \geq N_{iter}$. A flow sheet explaining the complete methodology is shown in Figure 3.2.

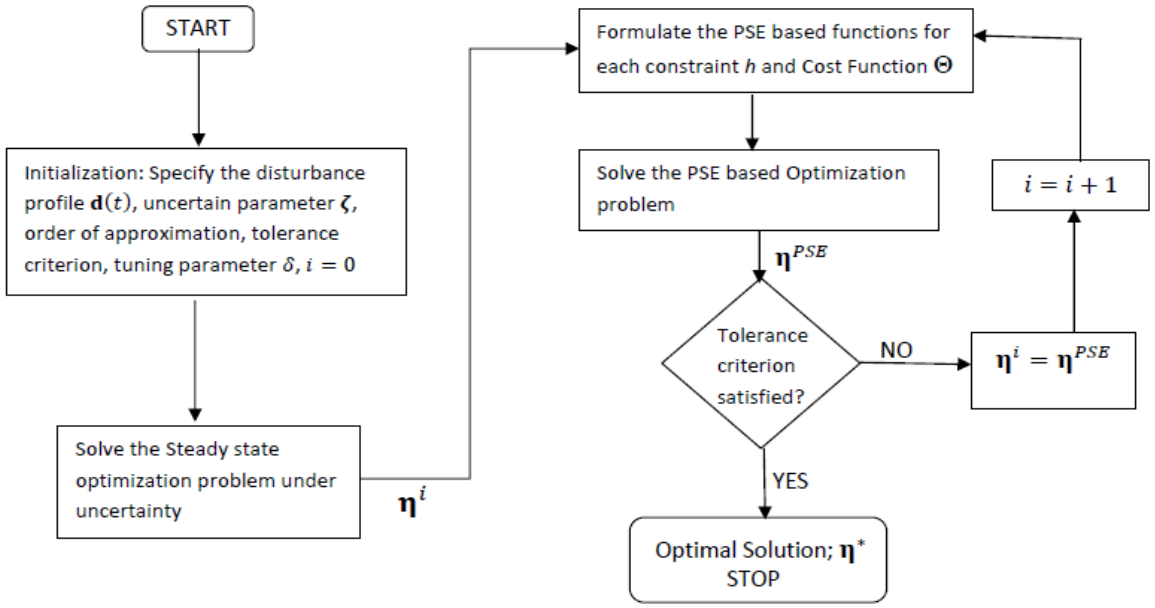

Figure 3.2 Flowsheet for the PSE based methodology

3.4 Remarks

The present methodology assumes that the process flow sheet and the control schemes remain fixed during the course of the calculations. Although structural (integer) decisions can be added into the analysis to consider the process topology, higher computational costs are expected. The simultaneous design and control of chemical processes featuring structural decisions are being considered as part of the future work in this research. The approach presented in this work assumes specific time-dependent disturbance profiles and discrete realizations in the uncertain parameters. Therefore, the case of stochastic descriptions defined for the disturbances and the uncertain parameters cannot be addressed with the present approach. Given their importance and significance, the formal use of stochastic descriptions for the disturbances and uncertain parameters is considered as part of the future improvements for the present methodology. As shown in equation (8), δ determines the size of the search space region in the optimization variables, i.e. $\boldsymbol{\eta}_{\text{nom}}(1-\delta) \leq \boldsymbol{\eta} \leq \boldsymbol{\eta}_{\text{nom}}(1+\delta)$. If large δ values are used, then the computational costs may be low; however, the search region around the nominal point will expand and PSE approximations may not be valid at that point thus leading to solutions that are sub-optimal or even cause a divergence in algorithm .On the other hand, using a relatively small δ value narrows the search direction in the optimization variables thus more surely resulting in identifying an optimal solution; however, the computational costs associated with this calculation may become significantly high due to the large number of iterations required to achieve such solution. It should be noted that the PSE based gradients can either be calculated analytically or numerically. In the present approach, analytical gradients can be calculated by integrating the original process models equations with an additional set of differential equations known as the sensitivity equations [48, 49]. On the other hand, the numerical computation of the gradients

requires sampling and introduces truncations errors in the calculations. While an analytical approach provides the true sensitivities of the process, the numerical approach is often preferred when the process is a black-box model or involves a large set of differential equations. The parameter N used for the convergence criterion also plays an important role in the present approach. If a small value of N is used, the cost function or the optimization variables might not converge. On the other hand, setting N to a large number will eventually converge at the expense of high computational costs. The step size in the finite difference method for the calculation of the gradients in the PSE functions is another key parameter. If a small step size is chosen, noise in the system increases affecting the quality of the gradients and therefore the PSE approximation. On the other hand, if a large step size is chosen, the sensitivity gradients calculated might not be accurate which will affect the accuracy of the PSE function and the optimization calculations. The big M values specified in problem (3.9), to penalize process constraints that are violated should be chosen carefully and a priori such that the set $\boldsymbol{\lambda}$ does not become part of the feasible solution once the proposed back-off method has converged. Relatively large M values might lead to ill conditioning of the optimization problem whereas small M values may not be sensitive enough to the overall cost function. The selection of the number of discrete points selected for the uncertain parameters will affect the computational costs and the quality of the solution. As the discrete realizations for the uncertain parameters increases, the computational costs will also increase. Also, the weights assigned to the corresponding discrete realization should also be carefully selected since they will directly determine the quality of the solution. Higher weights should be assigned to the realizations which have high probability of occurrence, e.g. the expected (mean) realizations in the uncertain parameters. Note that the dynamic performance of the actual system cannot be explicitly guaranteed using this approach since PSE-based functions are employed to

approximate the worst-case variability in time in the process constraints and the cost function due to specific realizations in the disturbances and uncertainty in the parameters. However, the PSE functions employed in this work are developed around the worst-case variability expected in the process constraints and cost function due to the realizations in the disturbances and uncertainty in the parameters (see Figure 3.1). Therefore, the present approach is implicitly considering the process dynamics behavior and through this means dynamic feasibility is assessed in the present approach. Accordingly, the optimal design and control scheme obtained by the present approach is able to guarantee dynamic feasibility only if the PSE functions employed are valid approximations to the actual process. The order of the PSE approximations used to represent the process constraints and the cost function also plays a vital role in the present algorithm. The higher the order of PSE approximation, the more accurate the approximations; however, this will also lead to higher computational costs. Generally, the order in the PSE approximation is chosen based on the nonlinearity present in the system and the desired accuracy in the optimal solution. There are two approaches that can be employed to determine the order of the PSE approximation. In the first approach, the order of the approximation is selected offline by performing trial-and-error simulations. The second method is a more formal approach in which the order of the PSE functions are calculated online, while implementing the back-off method, i.e. develop a PSE-function of a given order and determine its accuracy using the actual constraint function. An algorithm that can be embedded within the present methodology to determine online the order of the PSE-functions is presented in Figure 3.3. While the first approach reduces the computational costs, the second method is more accurate at the expense of using additional computational resources at each step in the proposed back-off methodology.

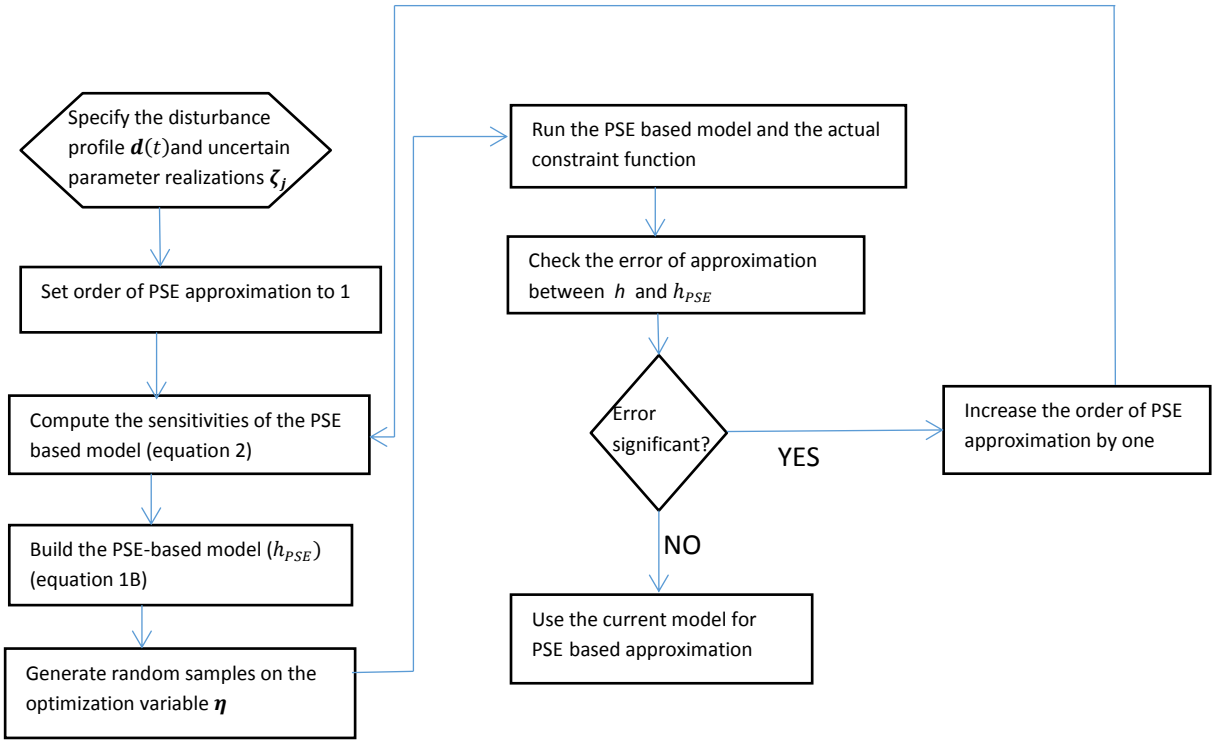

Figure 3.3: Procedure to select the order of the PSE

3.5 Case Study 1: Isothermal Mixing Tank

To illustrate the implementation of the methodology proposed in this work, the optimal design of an isothermal mixing tank is considered. Figure 3.4 shows the process flow sheet for this system. The step-by-step procedure describing the implementation of the methodology is described next.

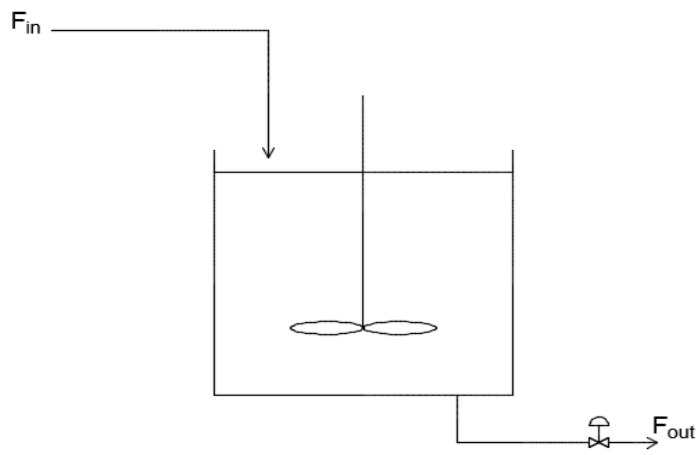

Figure 3.4 Flow sheet for Storage Tank

The process involves an inlet and an outlet stream. The system is assumed to be at constant temperature and density. The material balance for this system is as follows: [50]

$$A\frac{dH}{dt} = F_{in} - F_{out}$$

$$F_{out} = K\ Cv\sqrt{1.45 * 10^{-4}\beta g_0 \mathrm{H}} \qquad (3.13)$$

where A and H are the area and the height of the tank, respectively. The height of the tank represents the state variable in this process and it is assumed that this variable can be measured on-line. The term F_{in} is the inlet stream flow-rate and it is assumed to be a time-varying disturbance, i.e. **d**(t). The liquid level in the tank is controlled using the outlet stream flow-rate, F_{out}, which is defined as a non- linear function of the height (H) of the liquid level in the tank. Cv is the valve coefficient and is considered as an uncertain parameter in the system **ζ** , i.e. it is assumed that its true value is not known but it changes between lower and upper limits. The variable K represents the stem position of the valve at the outlet stream and it can be manipulated by a closed-loop controller to regulate the liquid level in the tank. A proportional–integral (PI) feedback controller is used in the present analysis to maintain the liquid level in the tank at a

desired set point (H_{sp}) by adjusting the stem position of the outlet valve (K). The terms β and g_0 represent the density of the fluid (water) and the standard gravity, respectively. The tank is assumed to be well mixed and with constant density. The constant term in equation (3.13) is a conversion factor. Table 3.1 lists the numerical data for this case study.

Table 3.1 Numerical Data for Storage Tank

Variable	Description
Inlet stream flow rate	$10gpm \leq F_{in} \leq 30gpm$
Outlet Valve Coefficient	$10 \leq Cv \leq 30$
Area of the tank	$A = 1m^2$
Density of the fluid	$\beta = 1000\ kg/m^3$
Proportional gain	$-0.1 \leq K_c \leq 1e-4$
Time integral	$0.5min \leq \tau_i \leq 10$

The goal in this process is to estimate the liquid level controller's set point, H_{sp}, and the PI controller tuning parameters, $K_c$and, τ_i, that minimize the cost of the tank. The final tank's volume must be such that it can accommodate the variations in the external process disturbances (F_{in}) and uncertainty in the process model parameters (C*v*) without overflowing or without having height's level below 5m (see equation (3.16) below). Thus, it is expected that the optimal controller's tuning parameters and liquid level set point will be those that reduce the maximum variability in the tank's liquid level, while complying with the process constraints. Therefore, the process design variable in this case is H, i.e. = **ω** = H.

K is the manipulated variable, which represent the controlled valve opening. Accordingly, the controllers' equation is as follows:

$$\mathrm{K}(t) = \bar{k} + K_c e + \frac{K_c}{\tau_i}\int_0^t e dt \quad (3.14)$$

where $\bar{k}$ represents the nominal value in the manipulated variable. K_c represents the controller's gain whereas τ_i is the controller's time integral, i.e. $\boldsymbol{\xi} = [K_c, \tau_i]$. Moreover, e is the error between the controlled variables, H and their corresponding set point, H_{sp}. The decision variables $\boldsymbol{\eta}$ included in the formulation are the height set point and the controllers tuning parameter, i.e. $\boldsymbol{\eta} = [H_{sp}, K_c, \tau_i]$.

Based on the above, the PSE based algorithm for simultaneous design and control was applied to this process. The capital cost for this process is assumed to be proportional to the tank's height H. Thus, the largest variation in the height of the tank with respect to the liquid level's set point at any time t determines the tank's capital cost. The largest variability in the tank's liquid level will result from a particular combination of a critical time-dependent profile in F_{in} and a critical steady-state unknown value in the valve's coefficient, Cv. The operating costs for this process are assumed to be negligible. Therefore, the cost function can be defined as follows:

$$\Theta_{ST} = 100H^{1.5} \quad (3.15)$$

The process constraints considered in the present analysis is the minimum allowable height in the tank at any time t, and the height of the tank should always be greater 5m; in addition, the stem opening must operate within its feasible operational limits. Therefore, the constraints considered for this process are as follows:

$$0 \leq \mathrm{K}(t) \leq 1$$

$$H(\mathrm{t}) \geq 5 \quad (3.16)$$

The step by step procedure used to implement the back-off methodology proposed in this work is discussed next.

Step 1: *Initialization*

The trajectory profile for the disturbances and the realization in uncertain parameters along with their respective weights are initialized first. The disturbance profile is assumed to be a series of step changes with the following nominal, lower and upper bounds:

$$\boldsymbol{d}(t)\text{: } F_{in}\left(\frac{\text{L}}{\text{min}}\right) = [6; 2.27; 6.81; 2.27; 6.81] \tag{3.17}$$

The first realization in the disturbance profile corresponds to the nominal value. The sampling time used for each realization in disturbances was set to 2,000 seconds. Likewise, each realization in the uncertain parameters along with their corresponding weights is shown in Table 3.2. Note that the nominal value for the valve coefficient (C*v*) is 20 and is assigned the maximum weight (See Table 3.2). A total of 5 realizations including the nominal value in the uncertain parameter is considered for this case study.

Table 3.2 Parameter Uncertain Description for Storage Tank

Valve's coefficient, C*v*.	Weights (w_j)
10	0.15
15	0.15
20	0.40
25	0.15
30	0.15

The tuning parameter δ determines the lower and upper bounds on the PSE-based optimization variables. That is, this parameter determines the size of the search space region in the PSE-based optimization problem and was set to 0.1. First and second order PSE approximation were considered and the results were compared. The maximum number of iterations (N_{iter}) was set to 400 whereas a tolerance criterion for convergence (ε) was set to 1 x10^{-4}; the parameter *M*, which represents a penalty cost in the PSE-based optimization problem, was set to 1x10^{6}. Further, the iteration index *i* is initialized to *i*=0.

Step 2: *Optimal steady-state design under uncertainty*

This step aims to find the optimal process design under uncertainty at steady state. The result obtained from the steady state design is then used as the initial guess in the present back-off methodology.

$$\min_{\boldsymbol{\eta}} \quad \sum_{j=1}^{J} w_j \, \Theta_{ST,j}(\boldsymbol{\eta}, \mathbf{d}, \boldsymbol{\zeta}_j)$$

Subject to:

$$\begin{aligned} & h_H^{min}(\boldsymbol{\eta}, \mathbf{d}, \boldsymbol{\zeta}_j) \leq 0 && \forall j = 1, \ldots, J \\ & h_K^{max}(\boldsymbol{\eta}, \mathbf{d}, \boldsymbol{\zeta}_j) \leq 0 && \forall j = 1, \ldots, J \\ & h_{K,PSE}^{min}(\boldsymbol{\eta}, \mathbf{d}, \boldsymbol{\zeta}_j) \leq 0 && \forall j = 1, \ldots, J \\ & \mathbf{d} = \{\mathbf{d}^l, \mathbf{d}^u\} \end{aligned} \qquad (3.18)$$

The formulation corresponds to the optimal design of a system using discrete realizations *j* in the uncertain parameters; hence, the multi-scenario approach has been used to solve this optimization problem. Note that in the present optimal steady state design formulation, the only optimization variable is the height of the tank H, i.e. $\boldsymbol{\eta} = \mathrm{H}$. The tank's height obtained from this problem represents the most economical steady-state design that can be accomplished under parameter uncertainty.

Step 3: *Develop the PSE-based functions*

Using the tank's height obtained from steady state design as the nominal operating point for the first (i^{th}) iteration, PSE-based functions are developed for each constraint h (i.e.h_{PSE}) considered in the formulation and also for the cost function. One example that describes the development of the PSE based functions is shown below. In order to explain this calculation, the constraint on the tank's height (3.16) is exemplified. This constraint can be reformulated according to the description presented in section 3.2 and is as follows:

$$h_H(t) \geq 5 \iff H_{min}(t) - \rho \geq 0 \iff -h^{min}_{H,PSE}(t) + 5 \leq 0 \qquad (3.19)$$

$H_{min}(t)$ is the maximum worst case deviation in the negative direction of the tank's height at any time t under process disturbances $\mathbf{d}(t)$ and parameter uncertainty $\boldsymbol{\zeta}$; ρ (5m) represents the input (saturation) limit on this constraint, i.e. the minimum allowed height of the tank during operation. PSE-based functions are developed for the reformulated constraint (3.16) for each iteration step i around the tank's height's nominal point $\boldsymbol{\eta}^i$, i.e. around nominal values in the optimization variables at the i^{th} iteration. First and second order sensitivity analyses were performed on each constraint and the cost function. The gradients are calculated using the finite difference method, more details regarding the computation of the sensitivities are provided in the first case study presented in the next chapter (See equations 4.16 and 4.17).

Step 4: *Optimization of the PSE-based functions*

The PSE based optimization problem for this case study can be formulated as follows:

$$\min_{\boldsymbol{\eta},\boldsymbol{\lambda}} \quad \sum_{j=1}^{J} w_j \, \Theta_{ST,j}(\boldsymbol{\eta}, \mathbf{d}(t), \boldsymbol{\zeta}) + \sum_{j=1}^{J} \sum_{s=1}^{S} M \, \lambda_{s,j}$$

Subject to:

$$h_{H,PSE}^{min}(\boldsymbol{\eta}, \mathbf{d}(t), \boldsymbol{\zeta}_j) + \rho \, (1 - \lambda_{1,j}) \leq 0 \qquad \forall j = 1, \ldots, J \qquad (3.20)$$

$$h_{K,PSE}^{max}(\boldsymbol{\eta}, \mathbf{d}(t), \boldsymbol{\zeta}_j) - \rho \, (1 + \lambda_{2,j}) \leq 0 \qquad \forall j = 1, \ldots, J$$

$$h_{K,PSE}^{min}(\boldsymbol{\eta}, \mathbf{d}(t), \boldsymbol{\zeta}_j) + \rho \, (1 - \lambda_{3,j}) \leq 0 \qquad \forall j = 1, \ldots, J$$

$$\boldsymbol{\eta}_{nom}(1 - \delta) \leq \boldsymbol{\eta} \leq \boldsymbol{\eta}_{nom}(1 + \delta)$$

$$\lambda_{s,j} \geq 0$$

where, $h_{H,PSE}^{min}$, and $h_{K,PSE}^{min}$ are the maximum deviation expected for the storage tank height and the valve's stem opening in the negative direction, respectively; similarly, $h_{K,PSE}^{max}$ is the worst-case variability expected for the stem opening in the positive direction. The solution to problem (3.20) ($\boldsymbol{\eta}^{i+1}$) represents an improvement in the search direction for the optimal design variable ($H_{sp}{}^{i+1}$) and controller tuning parameters ($K_c{}^{i+1}, \tau_i{}^{i+1}$), i.e. $\boldsymbol{\eta}^{i+1} = [H_{sp}{}^{i+1}, K_c{}^{i+1}, \tau_i{}^{i+1}]$**.** This is carried out in an iterative manner until one of the convergence criteria described in Step 5 in the algorithm is satisfied. λ is an optimization variable and represents the magnitude in the s^{th} constraint function $\mathbf{h}_{PSE}^{s}$ that is required to be added (removed) to avoid infeasibility. *M* represents a big number that needs to be degrees of magnitude higher than the actual cost function. Note that there is one $\lambda_{s,j}$ for each constraint function h_{PSE}^{s} and each realization in uncertain parameter $\boldsymbol{\zeta}_j$. It should be noted that the λ should be zero at the convergence point for the design and control parameters to be feasible under the given process dynamics and parameter uncertainty.

RESULTS

The case study presented in this work was coded on MATLAB 2014a using an Intel core i7 3770 CPU @3.4GHz processor (8GB RAM). Using the disturbance profile shown in equation (3.17) and for each realization is parameter uncertainty (Table 3.2) the results obtained for second order approximation are presented .The cost function and the decision variables are shown in Figure 3.5 and Figure 3.6: Decision Variable Convergence chart, respectively. The convergence of λ_s is shown in Figure 3.7. Validation of the process design obtained while using this approach is shown in Figure 3.8.

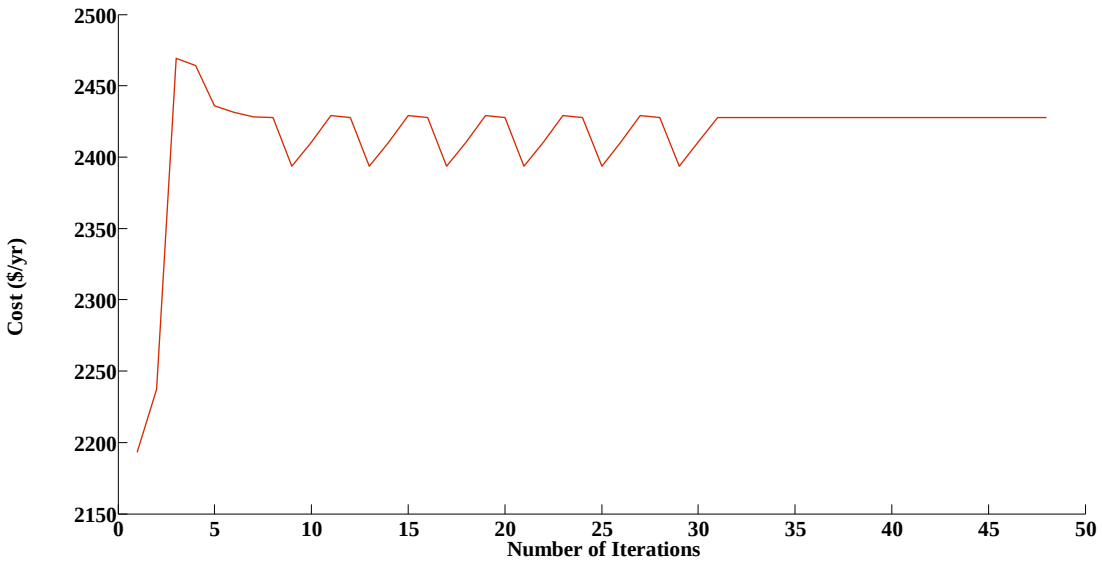

Figure 3.5: Cost Function Convergence chart

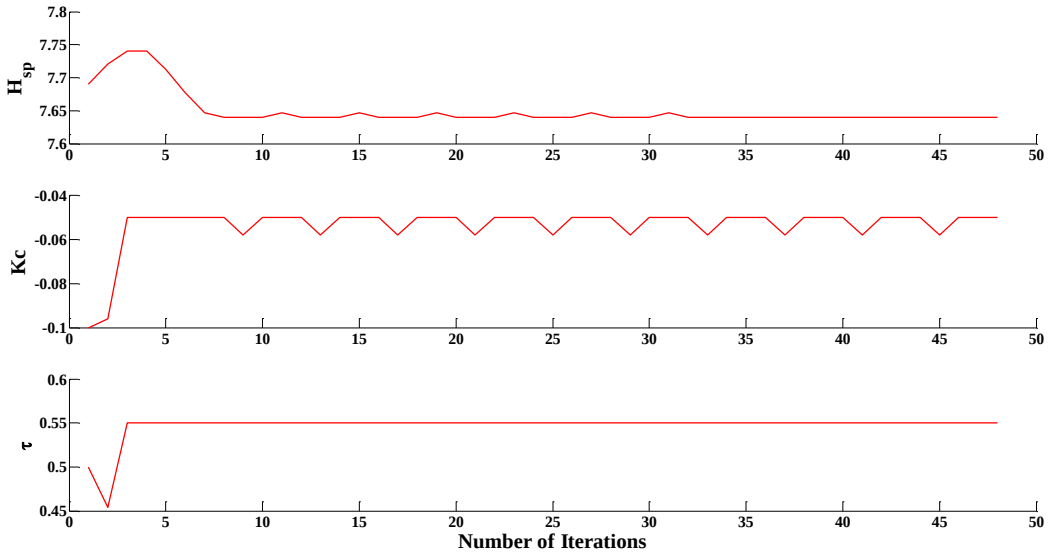

Figure 3.6: Decision Variable Convergence chart

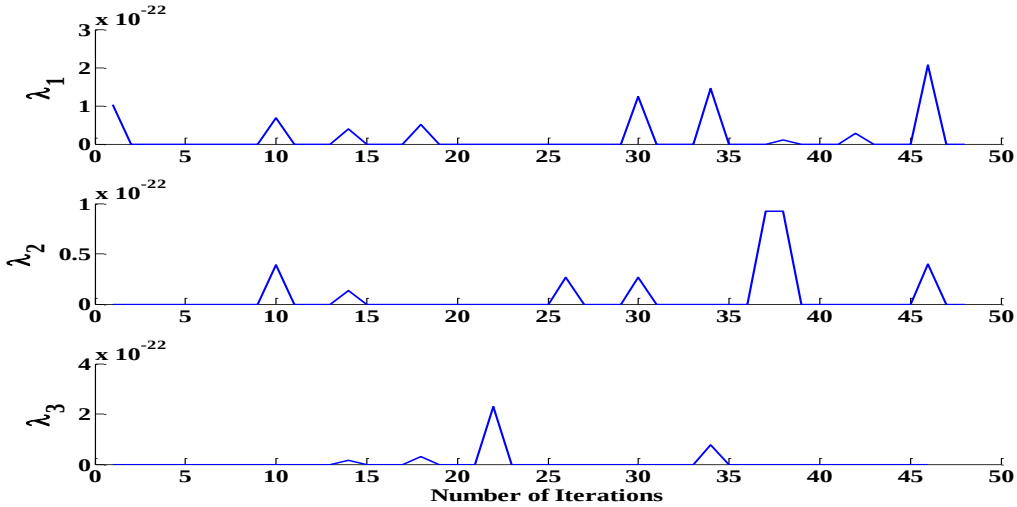

Figure 3.7: Convergence of λs

Fig 3.5 and 3.6 show that the cost function and the decision variables converged after 48 iterations. At the start of the simulation, large cost values are obtained. This is due to the fact that in this region some constraints are being violated when process dynamics are considered while using the optimal steady state design parameters as the starting point (see Step 2 above of the procedure). At these initial iterations, the λs were not equal to zero (See figure 3.7). The steady state cost when the dynamics of the system were not considered was $ 2192.86; the optimum cost value deviates from the optimal steady state design by around 10% when process disturbances and parameter uncertainty are considered in the system. The results obtained using the first and second order PSE approximation are presented in Table 3.3 and is also compared with the formal integration technique. The mathematical formulation for the formal integration technique is given in equation 3.21.

$$\min_{\boldsymbol{\eta}} \quad \sum_{j=1}^{J} w_j \, \Theta_{ST,j}(\boldsymbol{\eta}, \mathbf{d}(t), \boldsymbol{\zeta})$$

Subject to

Process model equations (equation 3.13)
Process constraints (equation 3.16) (3.21)
Disturbance dynamics (equation 3.17)
Parameter uncertainty (Table 3.2)

Table 3.3 Storage Tank Design Results

	PSE approximations 1st order	PSE approximations 2nd order	Formal integration technique
H_{sp}	7.91	7.67	7.97
K_c	0.013	0.05	0.062
τ_i	0.64	0.55	0.55
Total Cost ($/yr)	2,523.15	2,427.96	2,276.43
Computational Time (secs)	98	127	188

As shown in Table 3.3, a lower cost was obtained when second order PSE approximations are used. As the order increases, additional forward and backward points are required, which improve the quality in the results at the expense of additional computational costs, as observed in Table 3.3. The results obtained from the PSE based approach converges to an optimal design point that is somewhat similar to that obtained from the formal integration technique, i.e. less than 5% difference. It should be noted that, for the present case study, the computational time for the PSE-based approach is around 65% less than that for the formal integration technique. The result thus shows that the PSE based algorithm has the potential to obtain optimal design and control parameters in short computation times.

In order for the process constraints to be in their feasible limits, all the λ_s values should converge to zero, which can be seen in Figure 3.. As shown in Figure 3.8, the height of the tank H and the valve stem position K remained within their pre-specified operational limits in the presence of the process disturbances and parameter uncertainty considered for this case study. Each line in the

validation chart corresponds to a particular realization in uncertain parameter (See Table 3.2). This results thus show that the design parameters obtained from the PSE-based algorithm are dynamically feasible and returned a valid design.

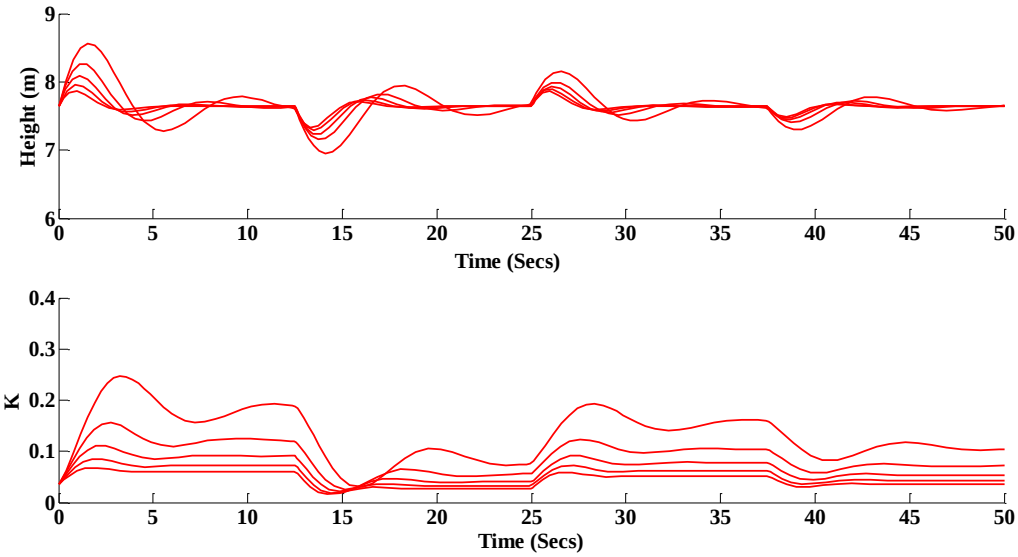

Figure 3.8: Simulating the design: Storage Tank Case Study

Summary

This chapter presented the novel approach proposed in this work for the optimal design of chemical processes in the presence of process disturbances and parameter uncertainty using Power Series Expansion (PSE) approximations. The methodology assumes that the process dynamic follows time dependent profiles specified as *a priori*. The idea in this work is to approximate the process constraint functions and process outputs using Power Series Expansion (PSE)-based functions in order to approximate the system and hence reduce computational costs. A step by step procedure to develop the PSE based optimization problem has been developed and presented in this section. In order to explain the methodology, a simple case study pertaining to the design of an isothermal

storage tank along with its results are shown. The results obtained from PSE based approach were compared with formal integration technique and it was shown that PSE based method can specify optimal process design and control schemes at low computational costs.

CHAPTER 4

Applications of PSE-based integration of design and control schemes: Case studies and results

The PSE-based integration of design and control methodology presented in the previous chapter has been tested using two different case studies. The first case study involves the optimal design of a non-isothermal CSTR under process dynamics and parameter uncertainty. The results from this case study have been compared with the formal integration technique in order to compare the computational cost of the new proposed methodology. The effect of various key parameters used in the methodology have been also discussed in detail. A waste water treatment plant, which is a large-scale complex process, was also designed using the proposed methodology and the results are presented in the later part of this chapter. The effect of tuning parameter and the type of disturbance profile used in the system has also been discussed in detail.

4.1 Non-isothermal Continuous Stirred Tank Reactor (CSTR)

In order to test the methodology proposed in the previous section, a case study involving the simultaneous design and control of a non-isothermal stirred tank reactor (CSTR) is considered. As shown in Figure 4.1, the reactor has a single input stream of reactant *A* which has a constant inlet concentration (C_{Ain}= 1mol/L). Time variant disturbances are considered in the inlet flow rate and the inlet temperature, i.e., $\mathbf{d}(t)= [q_F(t), T_f(t)]$.

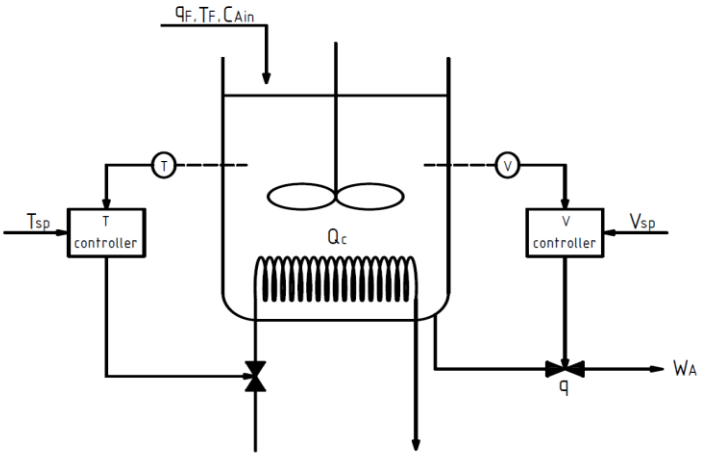

Figure 4.1: Schematic diagram of the CSTR closed-loop process.

An irreversible reaction takes place in the CSTR and the reactant *A* is converted into product *B*. Assuming a first order reaction is taking place, the rate of reaction can be given as follows:

$$-r_A = k_0 C_{Ar} \exp\left(-\frac{E}{RT_r}\right) \quad (4.1)$$

where C_{Ar} is the concentration of *A* in the reactor and T_r is the temperature inside the reactor; *E* is the activation energy and k_0 is the pre-exponential factor. Both the activation energy (E) and the pre-exponential factor (k_0) are considered to be uncertain parameters, i.e. $\boldsymbol{\zeta} = [k_0, \mathrm{E}]$. A cooling jacket is attached to the CSTR to regulate the temperature inside the system; Q_c is the cooling liquid flow rate inside the jacket whereas q and w_A are the reactor's outlet flow rate and the molar flow rate (mol/min) of reactant *A* at the outlet stream, respectively. The lower w_A, the more of the reactant is being converted into the product; hence, this variable can be used as a performance index for this system. The model equations for the mass and energy balances for this system are as follows [51]:

$$\frac{dV}{dt} = q_F - q \tag{4.2}$$

$$\frac{dT_r}{dt} = \frac{q_F(T_F - T_r)}{V} + \frac{\Delta H_0 k_0 C_{Ar} \exp\left(-\frac{E}{RT_r}\right)}{\rho C_P} - \frac{Q_c}{\rho C_P V} \tag{4.3}$$

$$\frac{dC_{Ar}}{dt} = \frac{q_F(C_{A,F} - C_{Ar})}{V} - k_0 C_{Ar} \exp\left(-\frac{E}{RT_r}\right) \tag{4.4}$$

$$Q_c = 48.1909 u_1 \tag{4.5}$$

$$q = 10 u_2 \sqrt{V} \tag{4.6}$$

The constants used in the above equations include the density of the fluid (ρ=1e3g/L), the heat capacity of the fluid (C_P=0.239J/gK), the heat of reaction (ΔH_0 =47.8 kJ/mol), and the universal gas constant (R=8.3144 J/molK). The control scheme considered for this CSTR includes two PI controllers, which manipulate the cooling liquid flow rate Q_c and the outlet stream flow rate q in order to regulate the temperature T_r and the liquid volume V inside the reactor. As shown in (4.5)-(4.6), u_1 and u_2 are the manipulated variables, which represent the controlled valve openings for Q_c and q, respectively. Accordingly, the controllers' equations are as follows:

$$u_1(t) = \overline{u_1} + K_{c1} e_1 + \frac{K_{c1}}{\tau_{i1}} \int_0^t e_1 dt \tag{4.7}$$

$$u_2(t) = \overline{u_2} + K_{c2} e_2 + \frac{K_{c2}}{\tau_{i2}} \int_0^t e_2 dt \tag{4.8}$$

where $\overline{u_1}$ and $\overline{u_2}$ are the nominal values in the manipulated variables. K_{c1} and K_{c2} represent the controllers' gains whereas τ_{i1} and τ_{i2} are the controllers' time integrals, i.e. $\boldsymbol{\xi} = [K_{c1}, K_{c2}, \tau_{i1}, \tau_{i2}]$. Moreover, $e_1$and e_2 are the errors between the controlled variables, V and T_r, and their corresponding set points, V_{sp} and T_{sp}. The decision variables $\boldsymbol{\eta}$ included the volume and temperature set points and the controllers tuning parameter, i.e. $= [V_{sp}, T_{sp}, K_{c1}, K_{c2}, \tau_{i1}, \tau_{i2}]$. Process constrains are applied to the temperature in the reactor T_r, the concentration of reactant A at the outlet stream C_{Ar} and the cooling water flow rate Q_c, i.e.

$$400 \leq T_r(t) \leq 480 \quad (4.9)$$
$$C_{Ar}(t) \leq 0.05 \quad (4.10)$$
$$Q_c(t) \leq 11 \quad (4.11)$$

As shown in (4.10) the concentration of reactant *A* in the outlet stream must be above 0.05 mol/L throughout the process time, which ensures a conversion of 95% or higher during the entire operation of this process. The cost function for this process (Θ_{CSTR}) considers the capital and variability costs, i.e.

$$\Theta_{CSTR} = \sum_{j=1}^{J} w_j \left(CAP_{CSTR,j} + VAR_{CSTR,j}\right) \quad (4.12)$$

where $CAP_{CSTR,j}$ is the capital cost of the reactor for the j^{th} realization in the uncertain parameters $\boldsymbol{\zeta}$. This cost is a function of the size of the reactor, i.e. height (*H*) and diameter (*D*). The dimensions of the reactor are calculated using the maximum (worst-case) variability expected in the reactor's volume hold up (V_{max}) due to time-dependent trajectory profiles in the disturbances and realizations in the uncertain parameters; w_j is the weight associated with the j^{th} realization in the uncertain parameters. Similarly, $VAR_{CSTR,j}$ represents the process variability costs and it is incurred due to the maximum variability in the molar flowrate of reactant *A* in the outlet stream, i.e. $w_{A_{max}}$. These cost correlations functions are expressed as follows:

$$CAP_{CSTR,j} = 1917r\left(D_j^{1.066} H_j^{0.802}\right)$$
$$VAR_{CSTR,j} = 105.12\, w_{A_{max,j}}$$
$$D_j = \left(0.03532\, V_{max,j}/4\pi\right)^3/2$$
$$H_j = 4D_j \quad (4.13)$$

where the term r represents the annualized rate of return on investment (r= 0.2). The operating cost due to steam consumption is negligible as compared to the capital and variable costs; hence, this cost is neglected from the process cost function.

The main objective of the case study is to minimize the total cost of the system by searching for the values in the process design parameters, i.e. V_{sp} and T_{sp}, and the controllers' tuning

parameters, $i.e. K_{c1}, K_{c2}, \tau_{i1}$ and τ_{i2}, that will maintain the dynamic operability of the process within its feasible limits at the lowest possible cost. The actual disturbance profiles defined in this case study are as follows:

$$\boldsymbol{d_1}(t)\text{: } q_F\left(\frac{\text{L}}{\text{min}}\right) = [200,150,150,250,250,150,250,150,250,150,250]$$
$$\boldsymbol{d_2}(t)\text{: } T_F(\text{K}) = [400,330,550,330,550,550,550,330,330,330,300] \quad (4.14)$$

Each realization in the uncertain parameters along with their corresponding weights is shown in Table 4.1. The first row in Table 4 are the nominal values for activation energy (E) and the pre exponential factor (k_0), respectively.

Table 4.1 Parameter uncertainty descriptions for CSTR

Activation Energy(E) (J/mol)	Pre Exponential factor(k_0)	Weights (w_j)
83,145	7.2e-10	0.4
1.10*83,145	1.10*7.2e-10	0.15
0.90*83,145	0.90*7.2e-10	0.15
0.90*83,145	1.10*7.2e-10	0.15
1.10*83,145	0.90*7.2e-10	0.15

The PSE based back-off methodology presented in the previous section was applied to this case study. The process model equations shown in (4.2) to (4.6) were used to search for the optimal steady-state design under the effect of process disturbances and parameter uncertainty. In this case, the critical scenarios assigned to the disturbances correspond to the different combination within their lower and upper bounds shown in (4.14).

In the next step, PSE-based functions were formulated for each of the process constraints shown in (4.9)-(4.11) and the cost function shown in (4.12). In order to explain this calculation, the constraint on the reactors concentration (4.10) is exemplified. This constraint can be reformulated according to the description presented in (3.1) as follows:

$$h_{C_{Ar}}(t) \leq 0.05 \Leftrightarrow C_{Ar_{max}}(t) - \rho \leq 0 \Leftrightarrow h^{max}_{C_{Ar},PSE}(t) - 0.05 \leq 0 \quad (4.15)$$

$C_{Armax}(\mathrm{t})$ is the maximum worst case variability of concentration of *A* inside the reactor at any time *t* under process disturbances **d**(t) and parameter uncertainty **ζ**; ρ $(0.05\ \mathrm{mol/L})$ represents the input (saturation) limit on this constraint, i.e. the maximum allowed concentration of species *A* during operation. PSE-based functions are developed for the reformulated constraint (4.15) for each iteration step *i* around the nominal point $\boldsymbol{\eta}^i$**,** i.e. around nominal values in the optimization variables at the i^{th} iteration. First and higher order sensitivity analyses were performed on each constraint and the cost function. Closed-loop simulations of the process were performed using the design and controllers equations (4.2) to (4.8), the disturbances' trajectory profiles shown in (4.14), and the realizations in the uncertain parameters shown in Table 4.1. If first-order sensitivity analysis is performed, seven closed-loop simulations will be required, i.e. one simulation using $\boldsymbol{\eta}_{nom}$ and six other simulations, one for each optimization variable considered in this study. Using (4.15), the worst-case deviation due to process disturbances and parameter uncertainty are calculated for the nominal and the forward step, i.e., $h^*_{C_{Ar}}|_{\boldsymbol{\eta}_{nom}}$ and $h^*_{C_{Ar}}|_{\eta^+_{p,j}}$, as shown in (3.4)-(3.5). These values can then be used to calculate the first order sensitivity terms of the PSE expansion for $h_{C_{Ar}}$. For example, the first-order sensitivity term with respect to T_{sp} can be calculated using forward finite differences, i.e.

$$Z^{(1)}_{T_{sp,j}} = \left(h^*_{C_{Ar}}|_{T^+_{sp,j}} - h^*_{C_{Ar}}|_{\boldsymbol{\eta}_{nom}}\right)/\left(T^+_{sp,j} - T_{sp_{nom}}\right) \quad (4.16)$$

where $T_{sp,j}^{+}$ and $T_{sp_{nom}}$ are the forward and the nominal values for T_{sp} at the i^{th} iteration step and at the jth realization in uncertain parameter. Similarly, second-order sensitivity analysis can be performed as shown in (3.7). Hence, the constraint for $h_{C_{Ar}}$ can be formulated as a PSE-based function as follows:

$$h_{C_{Ar},PSE}^{max}(t)|_{\mathbf{d}(t),\zeta_j} = h(\boldsymbol{\eta}_{nom}) + \sum_{p=1}^{P} Z_{p,j}^{(1)} \left(\eta_p - \eta_{p_{nom}}\right) + \sum_{p=1}^{P}\sum_{l=1}^{P} \frac{1}{2}\left(\eta_p - \eta_{p_{nom}}\right) Z_{pl,j}^{(2)} \left(\eta_l - \eta_{l_{nom}}\right) + \ldots \qquad (4.17)$$

As shown in equation (3.3), $Z_{p,j}^{(1)}$ and $Z_{pl,j}^{(2)}$ represent the first-order and second-order sensitivity for the constraint $h_{C_{Ar}}$ whereas η_p and η_l represent the p^{th} and the l^{th} elements in the decision variable vector $\boldsymbol{\eta}$.

The above procedure is employed to specify the rest of the PSE-based functions corresponding to each realization in the uncertain parameters for each constraint and the cost function. The next step in the present method is to formulate the PSE-based optimization problem:

$$\min_{\boldsymbol{\eta},\boldsymbol{\lambda}} \quad \sum_{j=1}^{J} w_j \, \Theta_{CSTR,j}(\boldsymbol{\eta}, \mathbf{d}(t), \boldsymbol{\zeta}) + \sum_{j=1}^{J}\sum_{s=1}^{S} M \, \lambda_{s,j}$$

Subject to:

$$\begin{aligned}
& h_{T_r,PSE}^{max}\left(\boldsymbol{\eta}, \mathbf{d}(t), \boldsymbol{\zeta}_j\right) - \rho\,(1 + \lambda_{1,j}) \le 0 && \forall j = 1, \ldots, J \\
& h_{T_r,PSE}^{min}\left(\boldsymbol{\eta}, \mathbf{d}(t), \boldsymbol{\zeta}_j\right) + \rho\,(1 - \lambda_{2,j}) \le 0 && \forall j = 1, \ldots, J \\
& h_{C_{Ar},PSE}^{max}\left(\boldsymbol{\eta}, \mathbf{d}(t), \boldsymbol{\zeta}_j\right) - \rho\,(1 + \lambda_{3,j}) \le 0 && \forall j = 1, \ldots, J \\
& h_{Q_c,PSE}^{max}\left(\boldsymbol{\eta}, \mathbf{d}(t), \boldsymbol{\zeta}_j\right) - \rho\,(1 + \lambda_{4,j}) \le 0 && \forall j = 1, \ldots, J \\
& \boldsymbol{\eta}_{nom}(1 - \delta) \le \boldsymbol{\eta} \le \boldsymbol{\eta}_{nom}(1 + \delta) \\
& \lambda_{s,j} \ge 0
\end{aligned} \qquad (4.18)$$

where, $h_{T_r,PSE}^{max}$, $h_{C_{Ar},PSE}^{max}$ and $h_{Q_c,PSE}^{max}$ are the maximum variability expected for the reactor's temperature, concentration and cooling water flow rate in the positive direction respectively; similarly, $h_{T_r,PSE}^{min}$ is the worst-case variability expected for the reactor's temperature in the negative

(decrease) direction. The PSE-based optimization problem shown in (4.18) is solved in an iterative manner until one of the convergence criteria described in Step 5 in the algorithm is satisfied. It should be noted that, for the optimization problem shown in (4.18), first or higher-order sensitivity analyses can be performed. Also, a key parameter in this algorithm is the tuning parameter δ. Sensitivity analyses on the effect of the tuning parameter δ and the order of the PSE approximations were performed and the results obtained are compiled below.

4.2 Results, Non-isothermal CSTR

The case study presented was solved under different scenarios. Each of these scenarios is discussed next. The case study presented in this work was coded on MATLAB 2014a using an Intel core i7 3770 CPU @3.4GHz processor (8GB RAM).

Scenario 1: Simultaneous design and control of the non-isothermal CSTR under the effect of disturbances

In this scenario, the optimal design and control parameters were identified using the disturbance profile specified in (4.14) whereas the uncertain process parameters shown in Table 4.1were assumed to be equal to their corresponding nominal values (first row in Table 4.1). Similarly, the tuning parameter δ was fixed to 0.03 and second order sensitivity analysis was employed. In the present analysis, the step size $\Delta\eta_p$used to compute the gradients was set to 0.005. The maximum number of iterations N_{iter} was set to 400 whereas the floating average convergence criterion described in Step 5 of the algorithm was used to stop the algorithm when a threshold value ε=1e-4 was reached. The cost function convergence chart and convergence charts for the optimization variables are shown in Figure 4.2 and Figure 4.3, respectively.

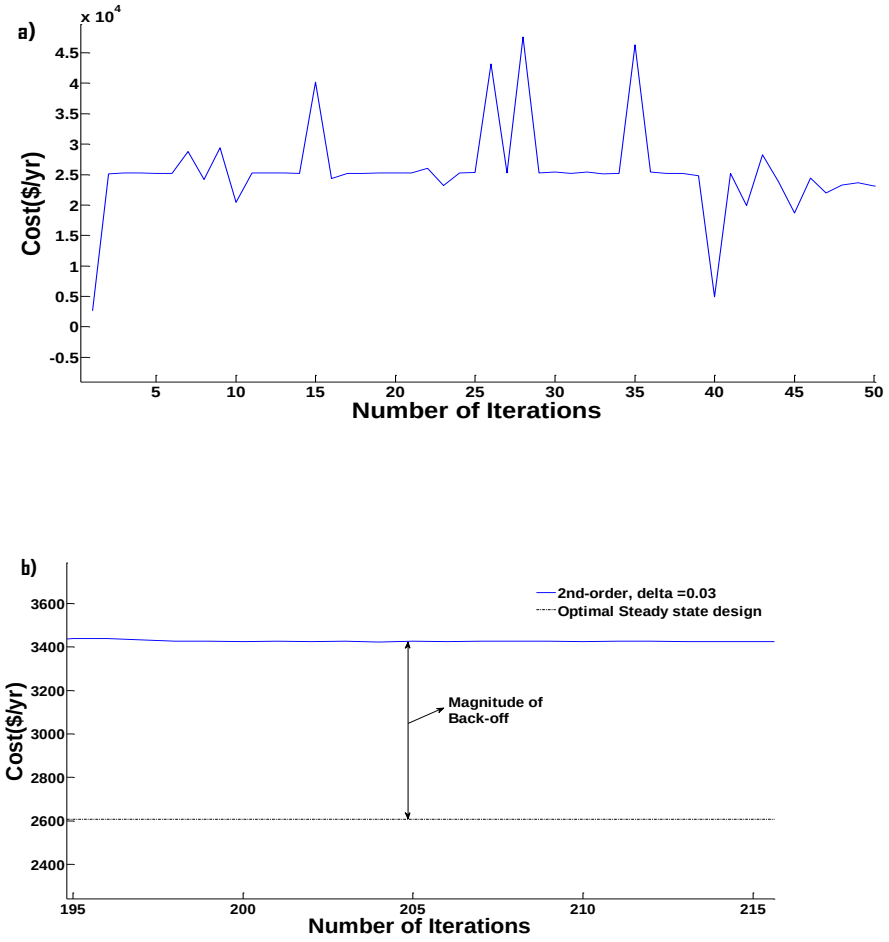

Figure 4.2 (a) Cost function chart for first 50 iterations; (b) Cost function for last 20 iterations

As shown in Figure 4.2 (b), the optimum cost value deviates from the optimal steady state design by around 30% when process disturbances are considered in the system. Similarly, all the optimization variables converged as it is shown in Figure 4.3(a). At the start of the simulation, large cost values are obtained as shown in Figure 4.2(a). This is due to the fact that in this region some constraints are being violated when process dynamics are considered for the optimal steady-state design ($\boldsymbol{\eta}_0$); hence, $\lambda_s > 0$ as shown in Figure 4.3b. The extra cost associated with it (i.e. $M\lambda_s$) is added up with the cost value hence resulting in a higher cost function values for the first few

iterations. As shown in Figure 4.3b, all the λ values corresponding to each process constraint converged to zero, indicating that the solution obtained is dynamic feasible under the given set of process disturbances. During the first 50 iterations, the magnitude by which the process constraints are been violated are relative high for the first constraint; therefore, large λ values are obtained from the optimization calculations for those iterations. As the iterations progress, the values in the design and control variables ($\boldsymbol{\eta}^{\mathbf{i+1}}$) moves away (back-off) from their corresponding steady-state point in a search direction that improves closed-loop dynamic feasibility; accordingly, the magnitude of all the λ's decreases and eventually converged to zero, indicating that a dynamically feasible solution while using the PSE-based approximation functions has been reached. A total of 216 iterations were needed to arrive at the optimal solution.

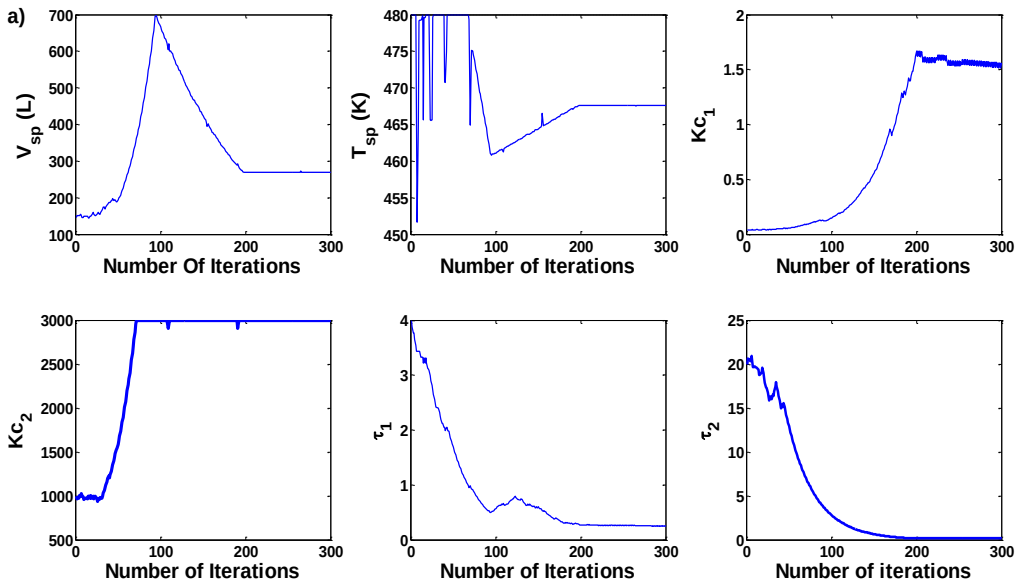

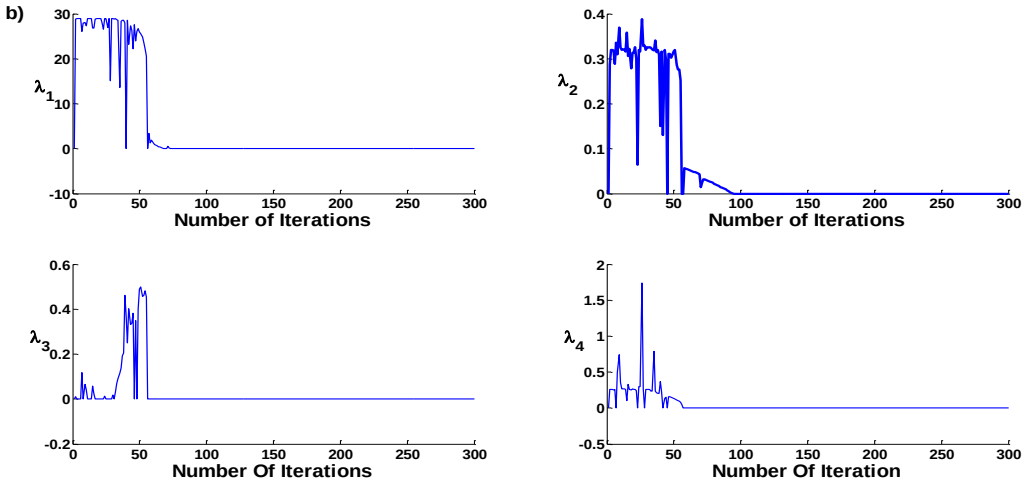

Figure 4.3: (a) Convergence of the optimization variables; (b) Convergence of λs

The results obtained from this scenario are compared with the formal integration of design and control technique in Table 4.2. In the formal integration approach, the problem aims to minimize the cost function and satisfy all the described process constrains under the process disturbances shown in (4.14) by solving all the process equations described in (4.2)-(4.8) and searching for the optimal values of the design and control optimization variables considered in the case study. Multiple initial points were considered in this formal integration of design and control approach including that obtained from the optimal steady-state design. As shown in Table 4.2 (Formal Integration: SS design), a higher cost is obtained when optimal steady state design was used as the initial point for the formal integration technique as compared to when other initial points were used for the formal integration technique. The results obtained from PSE-based method converge to a somewhat similar optimal design as that obtained from the formal integration process, i.e. less than $\pm$5% difference. However, the computational cost obtained from the proposed back-off approach is around 70% less as compared with the formal integration method (Table 4.2, Formal Integration: Multiple initial points). This result shows that, for the present case study, the back-off methodology based on PSE approximations is a promising economically attractive approach to

address simultaneous design and control. To validate the results, the design obtained from the PSE approach was simulated using the actual nonlinear dynamic model presented in (4.2)-(4.7) and the disturbance specification shown in (4.14). As shown in Figure 4.4, the concentration and temperature inside the reactor are maintained within their corresponding design limits in the presence of process disturbances. This shows that the design parameters obtained from the PSE-based approach are dynamically feasible.

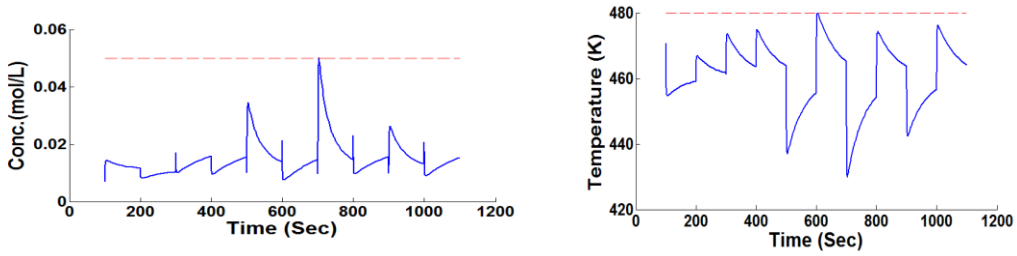

Figure 4.4 : Simulating the design: Temperature and Concentration profile inside the reactor

Table 4.2 Results: Scenario 1

	PSE based approach	Formal Integration:- Multiple initial points	Formal Integration:- SS Design
V_{sp} (L)	298.4	314.8	323.5
T_{sp} (K)	466.2	467.6	467.2
K_{c1}	1.52	1.49	1.34
K_{c2}	3000	3000	3000
τ_{i1}	0.38	0.57	0.64
τ_{i2}	0.12	0.34	0.31
Cost ($/yr)	3,446	3,512	3,587
PSE Iterations	216	--	--
Total CPU Time	1,045	3,345	348

Scenario 2: Effect of the tuning parameter δ

In this second scenario, the effect of tuning parameter δ on the quality of the solution and the computational costs are discussed. Simulations were conducted for δ =0.1, 0.2 and 0.3 using 2nd order PSE approximations. In order to study the effect of this parameter, the stopping criterion was turned off; instead, the algorithm was run for a maximum number of iterations, i.e. N_{iter}= 300. As shown in Figure 4.5(b), the solution obtained with δ=0.1 and δ=0.3 converged to different cost function values, which shows that selecting a suitable tuning parameter for this methodology is non-trivial and affects the overall performance of the algorithm. When δ is set to 0.3, the cost function converged to a value which is around 60% higher than the cost obtained when δ =0.1 (Table 4.3); similarly, the volume and temperature's set points converged to a different value as compared to the case when δ =0.1 or δ =0.2 (Figure 4.5c). When higher values of δ are used**,** there are sudden jumps (noise) in the decision variables and the cost function charts after every iteration, which can affect the quality of the solution (Figure 4.5a). These noises occur because the search region specified in the PSE-based optimization problem increases as δ is increased which might drive the search direction to different regions during the execution of the method. However, when δ is set to 0.1 the noise is reduced significantly and the results obtained are more accurate as compared to higher δ values.

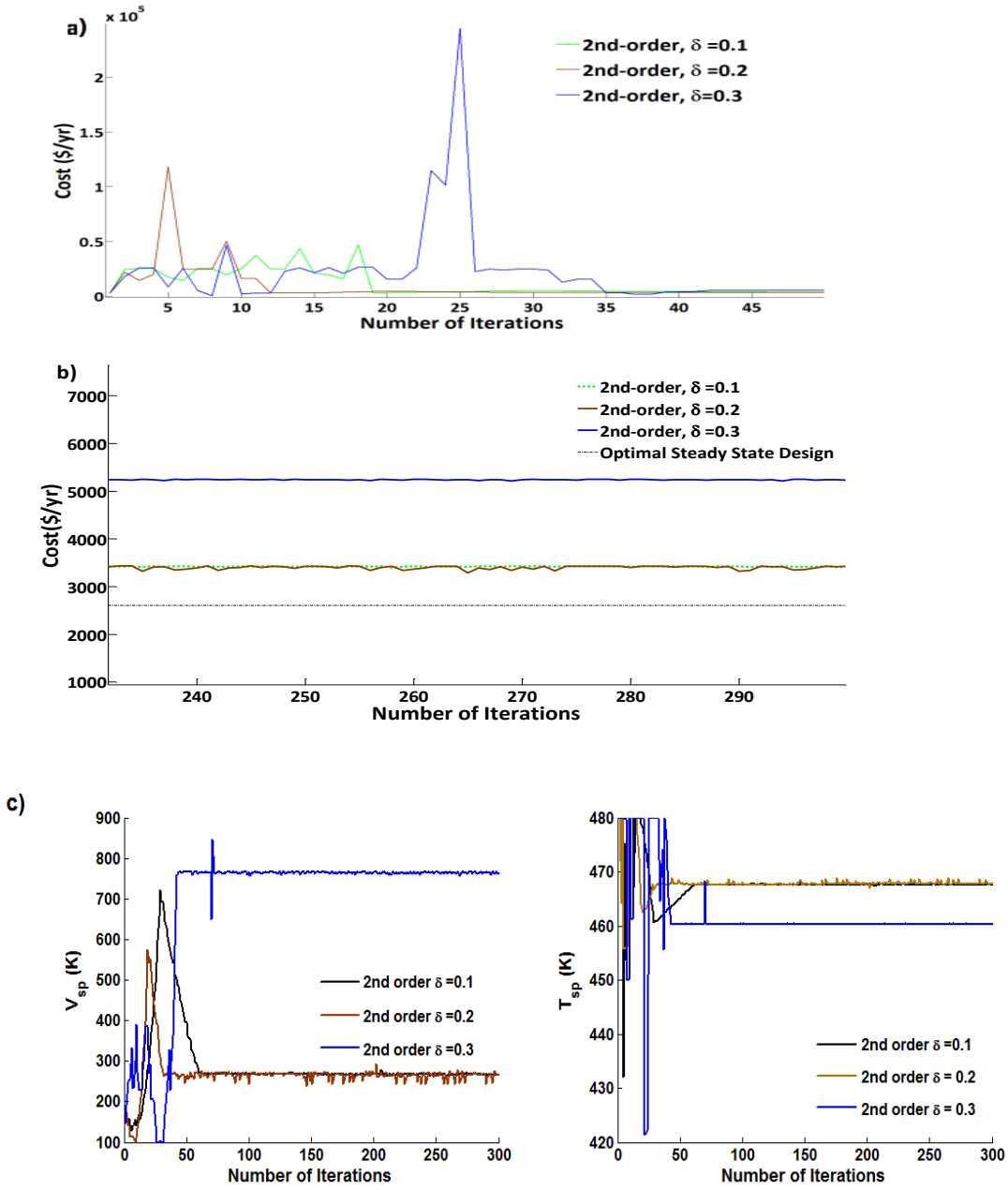

Figure 4.5 : (a) Cost function chart for first 50 iterations; (b) Cost function for last 50 iterations. (c) Volume and temperature's set points chart

Table 4.3 Results for different values of δ using Niter and the stopping criterion

	N_{iter}= 300			*Convergence criterion ON*		
	δ = 0.1	δ = 0.2	δ=0.3	δ = 0.1	δ = 0.2	δ = 0.3
V_{sp} (L)	287.6	297.3	745.7	288.2	298.7	744.6
T_{sp} (K)	462.3	465.8	466.2	462.1	465.4	465.7
Cost ($/yr)	3,482	3,487	5,276	3,471	3,476	5,282
PSE iteration	300	300	300	103	92	74
CPU time (s)	1,526	1,512	1,581	721	628	587

As shown in Table 4.3, the CPU time is similar in these cases since the algorithm was allowed to run for a maximum number of iterations using the same order in the PSE approximation. The results obtained when the convergence criterion described in Step 5 of the algorithm was used are also tabulated in Table 4.3 (Converge criterion ON). As shown in this table, the optimization parameters converged to the same point as compared when the algorithm was allowed to run for maximum number of iterations. It should also be noted that the computational time for δ =0.3 is almost 20% less than that recorded for δ= 0.1; however, accurate results were obtained when δ was set to 0.1.

Scenario 3: Effect of the power series approximation order

The order of the sensitivity used in the PSE functions can play a significant role in determining the quality of the results and the computational costs associated with the present approach. As the order increases, additional forward and backward points are required, which improve the quality in the results at the expense of using additional computational time. In this scenario, the effect of first, second and third order PSE approximations were analyzed while the tuning parameter δ was kept fixed at δ =0.1. The results obtained are presented in Table 4.4. All the simulations performed for different order of approximation resulted in somewhat similar designs, i.e. a difference of around $\pm$ 10%. The back off cost (last row: Table 4.4) represents the difference between the total

cost and the optimal steady state cost. As the order of the approximations increases, the quality of the result also increases. The improvement in the total cost by using higher order PSE approximation is majorly owing to expanding the power series expansion which results in a lesser back-off value. However, this is obtained at higher computational costs as additional iterations are required to converge to the optimal solution.

Table 4.4 Results obtained for different order of approximations

Optimization variables	1st Order	2nd order	3rd order
V_{Sp} (V)	304.8	298.7	296.7
T_{Sp}(K)	466.4	465.4	464.8
K_{c1}	1.89	1.69	1.28
K_{c2}	3000	3000	3000
τ_{i1}	0.51	0.41	0.32
τ_{i2}	0.26	0.18	0.14
PSE Iteration	64	92	174
CPU Time(s)	519	628	1,184
Capital Cost($/yr)	2,479	2,409	2,178
Variable Cost($/yr)	1,084	1,067	975
Total Cost ($/yr)	3,563	3,476	3,153
Total Cost, formal Integration	3,676	3,559	3,194
Error	3.07%	2.33%	1.28%
Back-off cost	1,833	1,746	1,423

In order to check the convergence of the results obtained by the present approach while using different orders in the PSE expansions, the results were used as initial points to perform the formal integration technique. As shown in Table 4.4, the error in costs reduces as high-order PSE expansions are used in the calculations. In addition, the errors are less than 3%, which confirms the convergence of the proposed back-off method within a certain tolerance error. Note that there is a significant change in cost when second order and third order approximations were used even

though the values obtained for V_{Sp} and T_{Sp} are approximately the same. However, the variability in the reactor's hold up is significantly reduced when third order PSE functions were employed in this approach. This is mostly due to the improvements in the tuning of the controller parameters. As the capital cost is a direct function of the reactor's maximum hold-up ($V_{max,j}$), the capital cost decreases by almost 10 % when third-order PSE functions are employed in the analysis. This result also demonstrates the key role control decisions play in the optimal design of dynamic systems under uncertainty.

Scenario 4: Effect of model parameter uncertainty

In the scenarios discussed above, only the effect of process disturbances was considered. In this scenario, both process disturbances and model parameter uncertainty are taken into consideration. As described before, the activation energy (E) and pre exponential factor (k_0) are the uncertain parameters for the present case study. These parameters were deviated by 10% of their nominal values and various combinations were used as parameter uncertainty (see Table 4.1). Second order sensitivity analysis was performed and the tuning parameter was set to δ=0.03. The maximum number of iterations was fixed to 300. The optimal design and controller parameters for this scenario along with the cost and CPU time are presented in Table 4.5. The cost obtained in this case is almost four times higher as compared to Scenario 1 when no uncertainty was introduced. The volume's set point also converged to a higher value (around ten times) as compared to Scenario 1. The total CPU time also increases by four times as simulations are now performed for each realization in the uncertain parameters. Figure 4.6 shows the time-based validation for this scenario using the actual nonlinear dynamic model presented in (13)-(19), the process disturbance specification shown in (26) and the realizations in the uncertain parameters shown in Table 4.1. As shown in this figure, the concentration and temperature inside the reactor are maintained within

their corresponding design limits. This demonstrates that the order of the PSE approximations employed for the present scenario are valid representations of the actual process constraints and cost function; therefore, dynamic feasibility is guaranteed for the specific disturbances and discrete realizations in the uncertain parameters considered in the analysis.

Table 4.5 Optimal design and controller parameters under parameter uncertainty

Optimization Variables	Level
V_{Sp}(V)	3,140
T_{Sp} (K)	465.3
Kc_1	0.13
Kc_2	3,000
τ_{i1}	1.03
τ_{i2}	3.87
Total Cost ($/yr)	13,250
Total CPU Time(s)	4,267

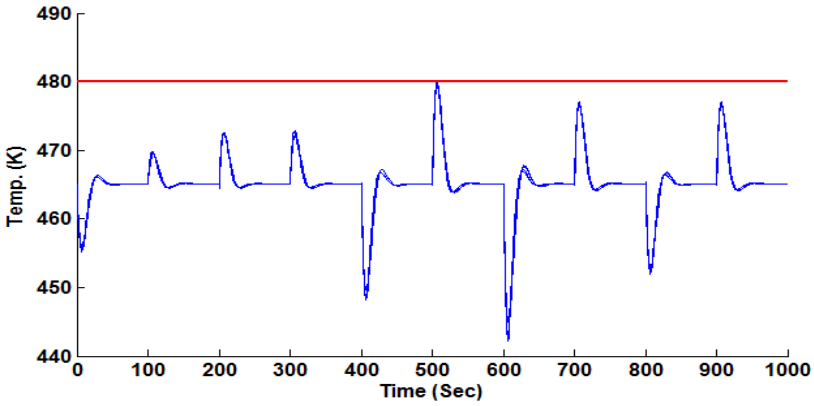

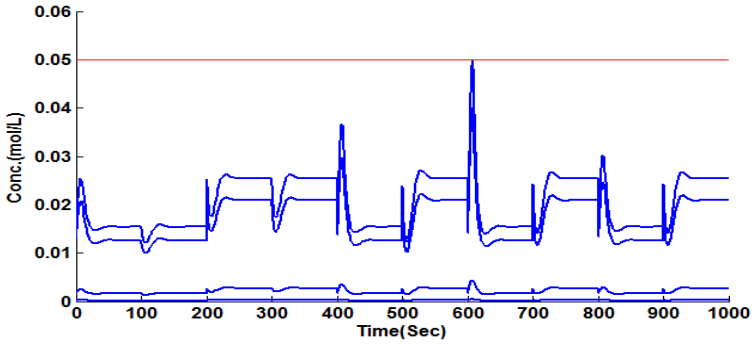

Figure 4.6: Simulating the design for each realization in process uncertainty. Concentration and temperature profile inside the reactor.

4.3 Waste Water treatment plant

In order to explore the potential of the PSE-based methodology for integration of design and control problems for large-scale complex chemical systems, the methodology proposed in this study has been tested on a waste water treatment plant. An existent activated sludge waste water treatment plant, located in Manresa, Spain was used for the present case study [20] .The activated sludge process is generally used for treating sewage and industrial wastewaters using air and biological components like bacteria and protozoa. A general flowsheet of the plant is shown in Figure 4.7 .

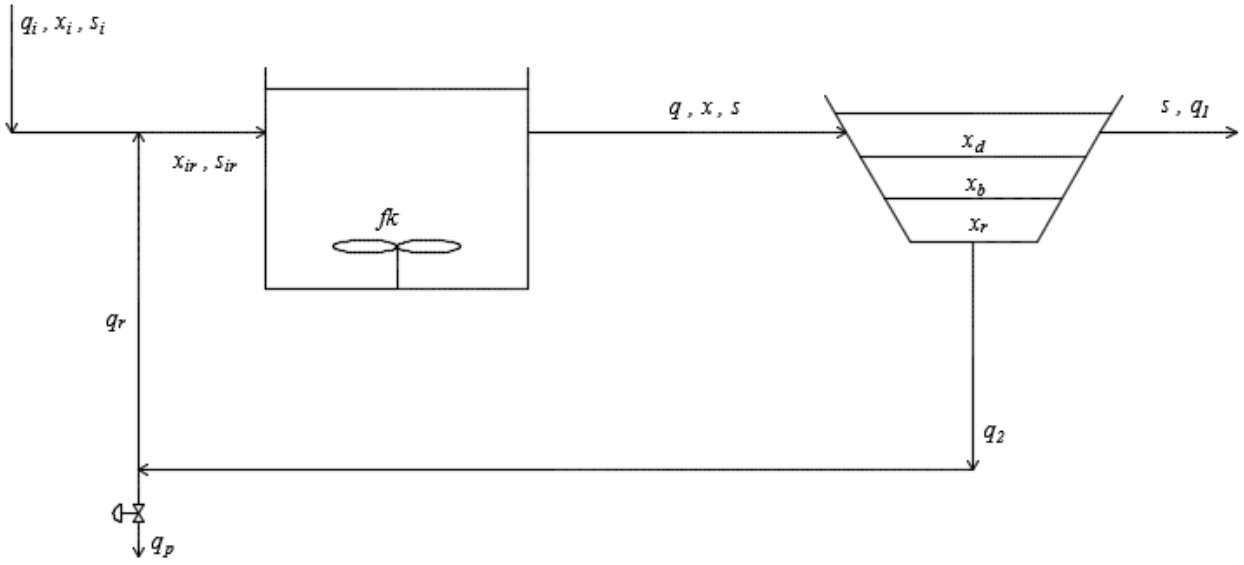

Figure 4.7 Schematic Diagram for waste water treatment plant

The plant consists of an aeration tank and a settling tank (clarifier) which are connected in series. The biomass, which is a biological matter that grows in the aeration tank due to consumption of organic matter, which is present in the treated effluent. The goal of this process is to regulate the level of the substrate concentration in the biodegradable effluent stream. Dissolved oxygen is supplied to the reactor through the aeration turbines. Water exiting the reactor flows to the corresponding settler where the activated sludge is separated from the clean water and is partially recycled back to the bio reactor. Part of the biomass is also removed from the system (as shown in Figure 4.7) to avoid excessive accumulation. The purged sludge is further treated by aerobic or anaerobic digestions for safe disposal. To simplify the analysis, only the activated sludge reactor and the clarification process shown in Figure 4.7 are modelled since they represent the most important units for this process. The rate of change of biomass and the rate by which the organic substrate is been consumed in the reactor are described as follows:

$$\frac{dx}{dt} = \mu y \frac{xs}{k_s+s} - k_d \frac{x^2}{s} - k_c x + \frac{q}{V}(x_{ir} - x) \quad (4.19)$$

$$\frac{ds}{dt} = \mu \frac{xs}{k_s+s} + f k_d \frac{x^2}{s} + f k_d k_c x + \frac{q}{V}(s_{ir} - s) \quad (4.20)$$

where x and s are the biomass and organic substrate concentrations (mg/L) inside the bioreactor, respectively; x_{ir} and s_{ir} are the the biomass and organic substrate concentrations (mg/L) entering the bioreactor, respectively; V is the volume of the reactor (m^3) and q denotes the bioreactors outlet flow (m^3/hr).

Since the concentration profile in the settler is a function of its depth, equations (4.21)-(4.23) describe the difference in settling rate between layers of different and increasing biomass concentration. Three layers were considered in this analysis which resulted in the following mass balance equations of biomass and oxygen:

$$\frac{dx_b}{dt} = \frac{1}{Alb}\left(q_i + q_2 - q_p\right)(x - x_b) - \frac{1}{lb}(vs(d) - vs(b)) \quad (4.21)$$

$$\frac{dx_d}{dt} = \frac{1}{Alb}\left(q_i - q_p\right)(x_b - x_d) - \frac{1}{ld} vs(d) \quad (4.22)$$

$$\frac{dx_r}{dt} = \frac{1}{Alb} q_2 (x_b - x_r) + \frac{1}{lr} vs(b) \quad (4.23)$$

$$\frac{dc}{dt} = k_{la} f k (c_s - c) - OUR - \frac{q}{V} c \quad (4.24)$$

$$OUR = k_{01} \mu x \frac{x}{k_s+s} \quad (4.25)$$

$$q_1 = q - q_2 \quad (4.26)$$

$$q_r = q_2 - q_p \quad (4.27)$$

$$q = q_i - q_r \quad (4.28)$$

where x_d, x_b, x_r are the biomass concentrations (mg/L) at the different layers in the clarifier unit, i.e. surface, intermediate and bottom, respectively; ld, lb and lr are the depth of the first, second and the bottom layer in the settler whereas $vs(d)$, $vs(b)$ and $vs(r)$ refer to the rate of settling for

the activated sludge and its changes from layer to layer and depends on the concentration of biomass in those layers. Dissolved oxygen in denoted by c, which is supplied by the aeration turbines. The speed of these aeration turbines is denoted by fk. The volume of the aeration tank is given by V(m^3); the rest of the parameters, and their corresponding nominal values, are described in Table 4.6.

The control problem consists of maintaining the substrate concentration (s) in the bioreactor and to maintain the dissolved oxygen concentration (c) in the settler at the desired levels in presence of process disturbances corresponding to the change in the feed rate (q_i), inlet concentration of the substrate (s_i) and the biomass concentration in the inlet feed (x_i).

Table 4.6 Description of model parameters

Symbols	Description	Value
μ	Specific growth rate	0.1824(hr^{-1})
y	Fraction of converted substrate to biomass	0.5948
k_s	Saturation constant	300(hr^{-1})
k_d	Biomass death rate	5E-5(hr^{-1})
k_c	Specific Cellular activity	1.33E-4(hr^{-1})
k_{la}	Oxygen transfer into the water constant	0.7(hr^{-1})
k_{01}	Oxygen demand constant	1.00E-4 (hr^{-1})
c_s	Oxygen specific saturation	8.0 (hr^{-1})
fk_d	Fraction of death biomass	0.2

Cost function

For the present case study, the annualized capital cost of the plant (CC) is given by the size of the bioreactor (V) and the cross sectional area of the decanter (A); i.e.,

$$CC = 364(1000V + 350A) \quad (4.29)$$

The volume (V) and the area (A) are the decision variables in the optimization problem. The annual operating cost for the system (OC) will depend by the amount the energy consumed by the aeration turbines and the pumps used for purging, i.e.

$$OC = 15fk + 0.8qp \quad (4.30)$$

One of the key objectives of this process is to maintain the substrate concentration below a certain threshold. Since the substrate contains toxic components and any increase in the concentration from the desired level leads to high penalty cost. Therefore, a dynamic variability cost (VC) is considered for this variable; this variability cost is defined as a function of the largest variability observed in the substrate concentration throughout the process, i.e.

$$VC = 10^5 s_{max}(t) \quad (4.31)$$

where s_{max} is the largest variability in the substrate concentration at any time t. Note that a higher variable cost is assigned to the variability in the substrate concentration because of the environmental significance and restriction in having higher concentration of the substrate in the treated water to the effluent. Therefore, the annual total cost (Θ_{WW}) for this process is as follows:

$$\Theta_{WW} = CC + OC + VC \quad (4.32)$$

The following process constraints are considered for this process:

$$0.01 \leq \frac{q_p(t)}{q_2(t)} \leq 0.2$$

$$0.8 \leq \frac{V.x(t)+A.lr.x_r(t)}{q_p.x_r(t).24} \leq 15$$

$$s(t) \leq 100 \quad (4.33)$$

The first two constraints shown in equation (4.33) represents the feasible limits on the ratio between the purge to the recycle flow rates and the purge age in the decanter. The last constraint

in equation (4.33) refers to the maximum allowable substrate concentration in the treated water that leaves the classifier. It should be noted that all the three process constraints should be within their feasible limits during operation. These process constraints along with the cost function will be approximated using the PSE functions as described in the section 3.2 The control scheme considered for this case study includes two PI controllers that regulate the substrate concentration and the dissolved oxygen. The manipulated variables considered for the system are the purge flow rate (q_p)and the turbine speed (fk) respectively. The controller gain K_{c1} and time constant τ_{i1} corresponds to the controller that regulates the substrate s in the system whereas K_{c2} and τ_{i2} corresponds to the dissolved oxygen c control loop.

4.4 Results, waste water treatment plant

The case study presented in the previous section was solved under different scenarios. Each of these scenarios is discussed next. The case study presented in this work was coded on MATLAB 2014a using an Intel core i7 3770 CPU @3.4GHz processor (8GB RAM).

Scenario 1: Simultaneous design and control under the effect of step disturbances

The optimal design and control was performed using step changes as disturbance profiles whose nominal, upper and lower bounds are specified in equation (4.34). The three disturbances in the system are the inlet feed rate (q_i), inlet concentration of the substrate (s_i) and the biomass concentration in the inlet feed (x_i).The first realization in the disturbances corresponds to the nominal values. The sampling time for each step change in the disturbances was performed every 2,000 seconds.

$$\boldsymbol{d_1}(t)\text{: } q_i\left(\frac{m^3}{\text{hr}}\right) = [500, 480\ ,520, 480, 500\ ,520\ ,520]$$

$$\boldsymbol{d_2}(t)\text{: } x_i(\frac{mg}{L}) = [366\ ,371\ ,361, 366, 371\ ,366, 366]$$

$$\boldsymbol{d_3}(t)\text{: } s_i(\frac{mg}{L}) = [80\ ,75, 85\ ,80\ ,75,85\ ,80] \quad (4.34)$$

In the analysis, the maximum number of iterations N_{iter} was set to 400 whereas the floating average convergence criterion described in Step 5 of the algorithm to stop the algorithm was set to ε=1e-2. There were nine decision variables in the system. The decision variables include the area (A), Volume (V), nominal value for the biomass concentration x_{nom}, the substrate set point s_{sp} , the dissolved oxygen concentration set point C_{sp} and the tuning parameters for the 2 PI controllers.

In order to obtain a suitable tuning parameter δ for this case study, the effect of the tuning parameter on the optimal process design and control scheme configuration was studied first. Four different δ values were chosen offline and compared. The cost function convergence chart for different δ values is shown in Figure 4.8.

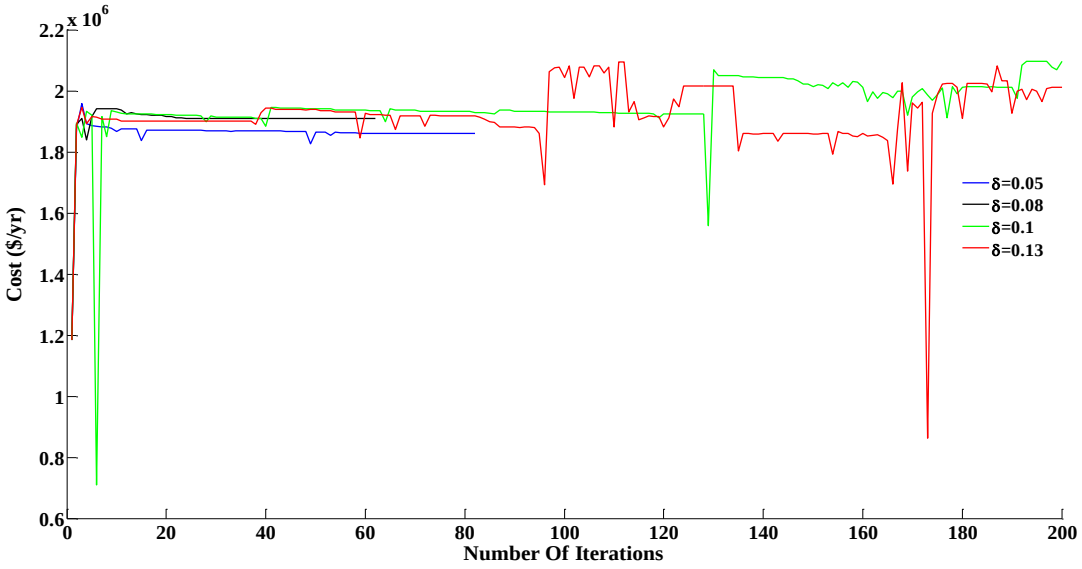

Figure 4.8: Cost function convergence chart for different tuning parameters

As shown in Figure 4.8, simulations were conducted for δ =0.05, 0.08, 0.1 and 0.13 using 2nd order PSE approximations. The maximum number of iterations N_{iter} was set to 200. As shown in Figure 4.8, the system converged after 82 and 62 iterations when δ=0.05 and δ=0.08, respectively. It should be noted that when δ=0.05, the algorithm required a larger number of iterations to converge but a lower cost ($1.86E+06/yr) was achieved when compared with δ=0.08 ($1.93E+06/yr). When higher values are used, the search region increases and the system converged to a different point. The system did not converge after 200 iterations when δ=0.1 and 0.13 were used, which indicated that these values will not be a suitable tuning parameter value for this case study as the search region is expanded when those values are used. The system might not have converged because the PSE approximations may no longer be valid for wider search space regions. Furthermore, these results matches with the conclusion drawn from the previous case study (Section 4.2) that high

noise is detected when higher δ values are used and therefore drive the optimal search direction to different regions during the execution of the method.

Since the lowest cost was obtained when δ was set to 0.05, this value was fixed for the rest of the studies conducted for the present case study. Detailed results using $\delta = 0.05$ are shown in Table 4.7 for 2nd order PSE approximations (Scenario 1). Note that the sensitivities were calculated using the finite difference method as described in section 4.1 for the CSTR case study.

Table 4.7 Results for different scenarios

Optimization variable	Scenario 1	Formal Integration	Scenario 2	Scenario 3
Area (m^2)	1,397.6	1,641.2	1,441.7	1,545.4
Volume(m^3)	1,121.6	1,186.8	1024.3	1,021.2
x	2,659.8	2,589.6	2,712.5	2,682.1
s_{sp}	93.66	93.14	99.7	93.4
C_{sp}	0.022	0.023	0.034	0.04
K_{c1}	0.09	0.32	0.27	0.07
K_{c2}	0.07	0.07	0.133	0.087
τ_{i1}	3.75	6.54	4.81	4.45
τ_{i2}	6.75	10.1	11.25	13.53
Total Cost($/yr)	1.785 E+06	1.9376 E+06	1.3497E+06	2.0637 E+06
Iterations	42	-	122	62
Total CPU Time (secs)	225	543	457	1865

The cost function convergence chart and convergence charts for the optimization variables are shown in Figure 4.9 and Figure 4.10, respectively. The optimum cost value deviates from the optimal steady state design by around 60% when process disturbances are considered in the system (See Figure 4.9). As shown in Figure 4.10, the volume (V) are higher and the s_{sp} is lower for the first few iterations which also increases the cost value for the first few iterations which can be noticed in Figure 4.9. The cost function converged after 42 iterations when the convergence criteria shown in step 5 of algorithm was used.

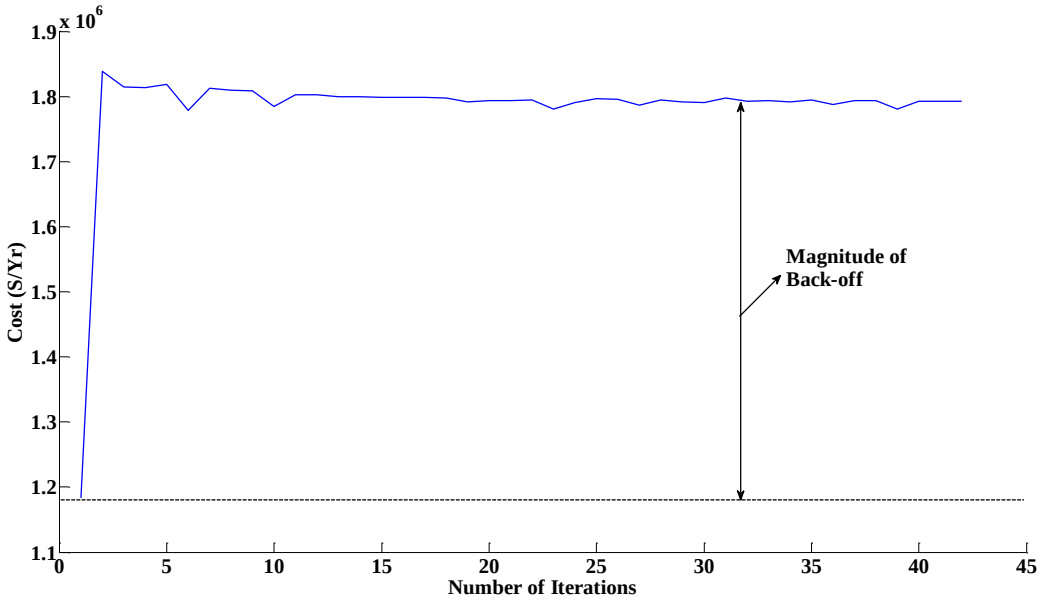

Figure 4.9. Scenario 1: Cost function convergence chart. Black line shows the optimal steady state cost.

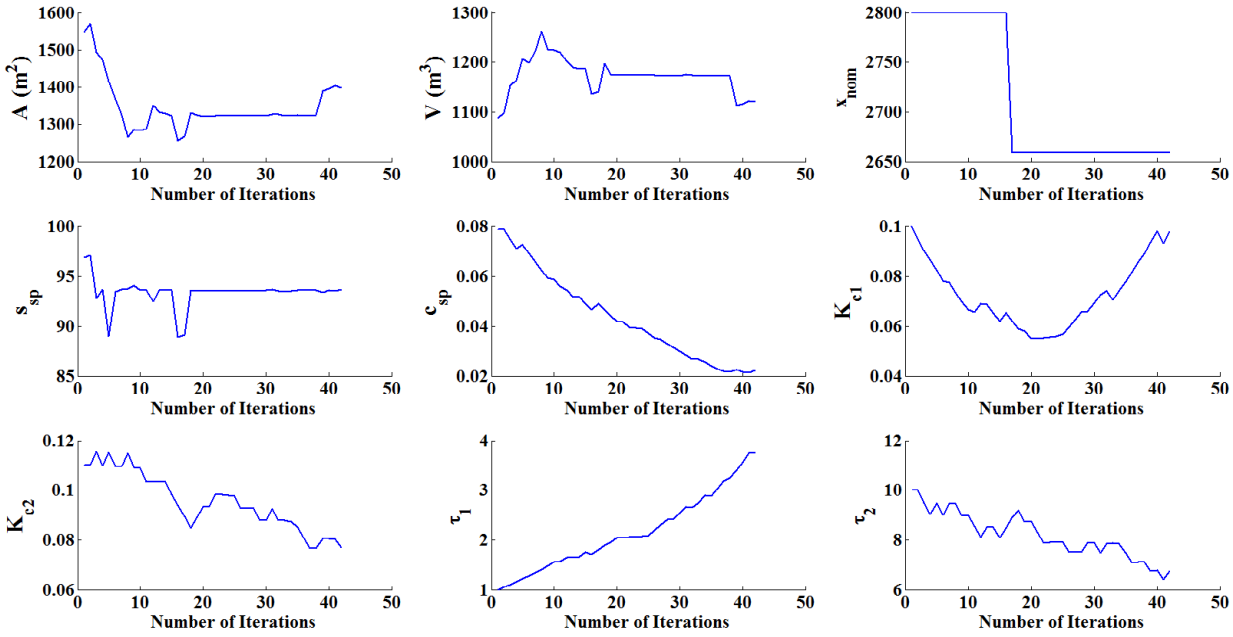

Figure 4.10: Scenario 1: Convergence of the optimization variables

The results were also compared with the formal integration technique and are shown in Table 4.7 (Formal Integration). The mathematical model for the formal integration technique is as follows:

$$\min_{\boldsymbol{\eta}} \quad \Theta_{WW}\left(\boldsymbol{\eta}, \mathbf{d}(t)\right)$$

Subject to Process model equations (equations 4.19- 4.28)
Process constraints (equation 4.33) (4.35)
Process Dynamics (equation 4.34)

As shown in Table 4.7 (Formal Integration), a higher cost of about 8% is obtained when the formal integration technique was used as compared with the PSE based approach. A difference of 8% was noticed because initial guess used in formal integration technique was the steady state optimization solution under uncertainty. If multiple initial guesses are used, a more optimal solution can be

found. A more optimal solution u It should be noted that since the substrate set point s_{sp} converges to a lower value when formal integration technique is used, higher cost is obtained in this case when compared with PSE based method. However, the computational cost obtained from the proposed back-off approach is around 60% less as compared with the formal integration method. This result shows that, for the present case study, the back-off methodology based on PSE approximations is a promising computationally attractive approach to address simultaneous design and control for large-scale complex systems.

The CPU time required for this case study was found to be higher compared with the CSTR case study which is discussed before (Table 4.2). This is due to the fact that the waste water treatment plant is a more complex and highly non-linear when compared with the CSTR problem. Therefore, the CPU time is expected to increase with increase in the degree of non-linearity in the system. Figure 4.11 shows the dynamic validation for the system. As shown in this figure, the substrate concentration, the ratio between the purge to the recycle flow rates and the purge age in the decanter remained within their corresponding operational limits in the presence of step changes in the disturbances. Note that the constraint which bounds the substrate is the only active constraint in the system.

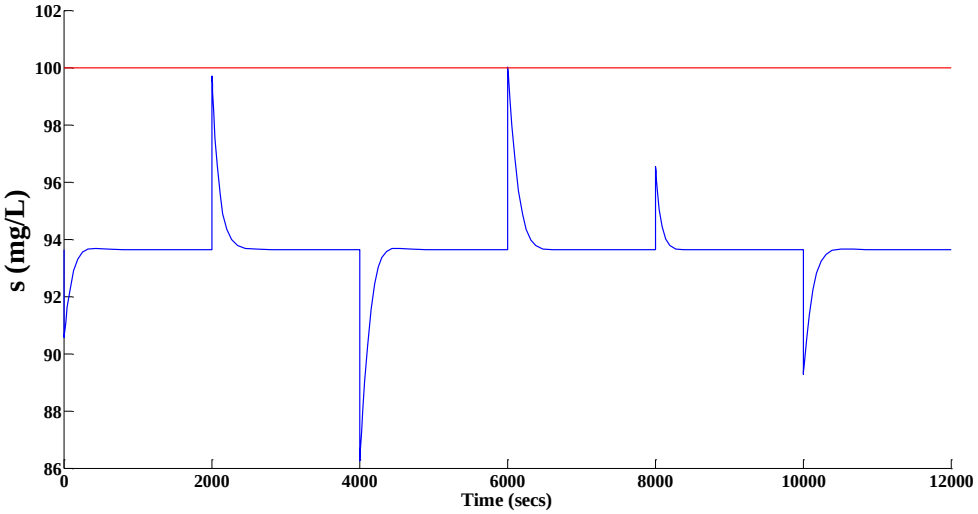
s (mg/L)
Time (secs)
102
100
98
96
94
92
90
88
86
0
2000
4000
6000
8000
10000
12000

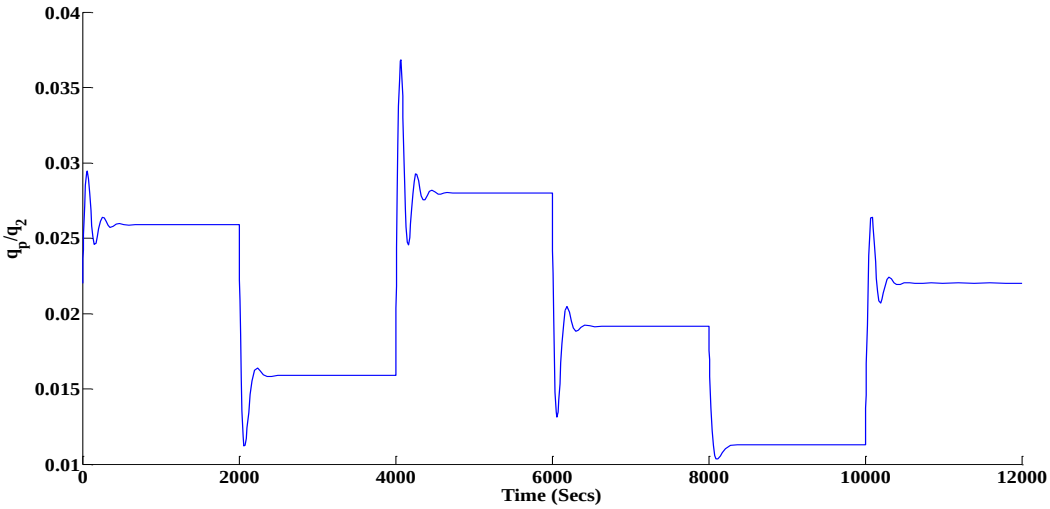
q_p/q_2
Time (Secs)
0.04
0.035
0.03
0.025
0.02
0.015
0.01
0
2000
4000
6000
8000
10000
12000

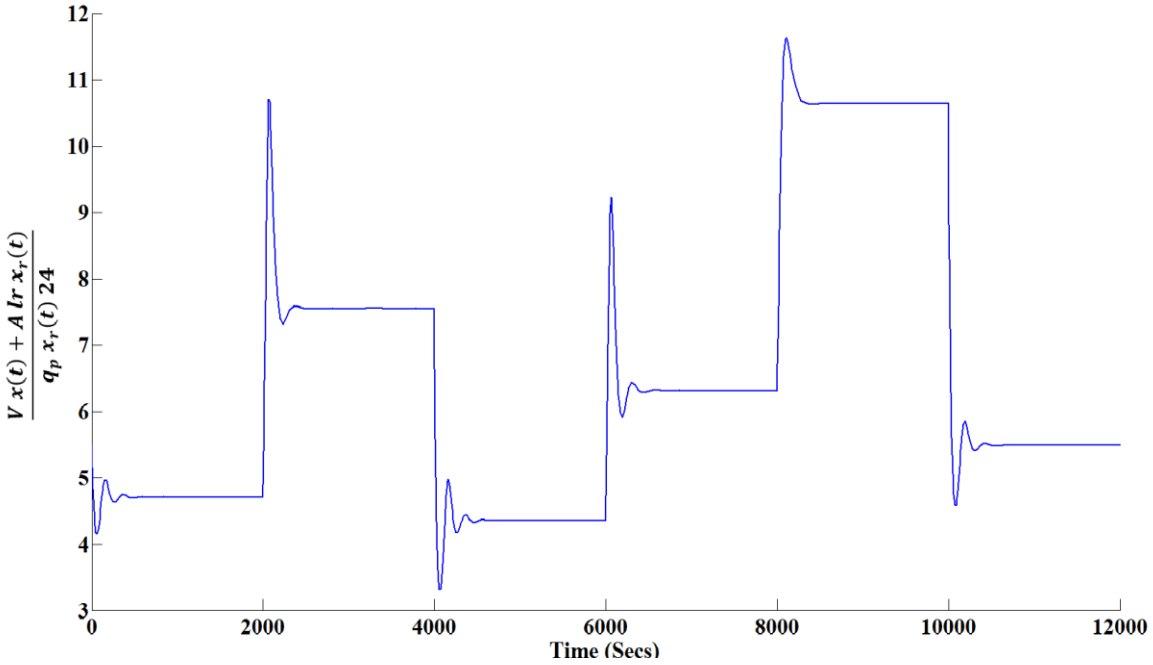

Figure 4.11 Simulating the Design, Scenario 1

Scenario 2: Simultaneous design and control under the effect of ramp disturbances

In this scenario, the optimal design and control was performed using ramps as the dynamic profiles for each of the disturbances considered in the present analysis (see Figure 4.12). During the ramp changes, the rate of change for inlet feed rate (q_i) is maintained at 20 $\left(\frac{m^3}{\text{hr}}\right)$ for a period of 1,000 seconds and for the inlet concentration of the substrate (s_i) and the biomass concentration in the inlet feed (x_i) the rate of change is 5 ($\frac{mg}{L}$) for a period of 1,000 seconds.

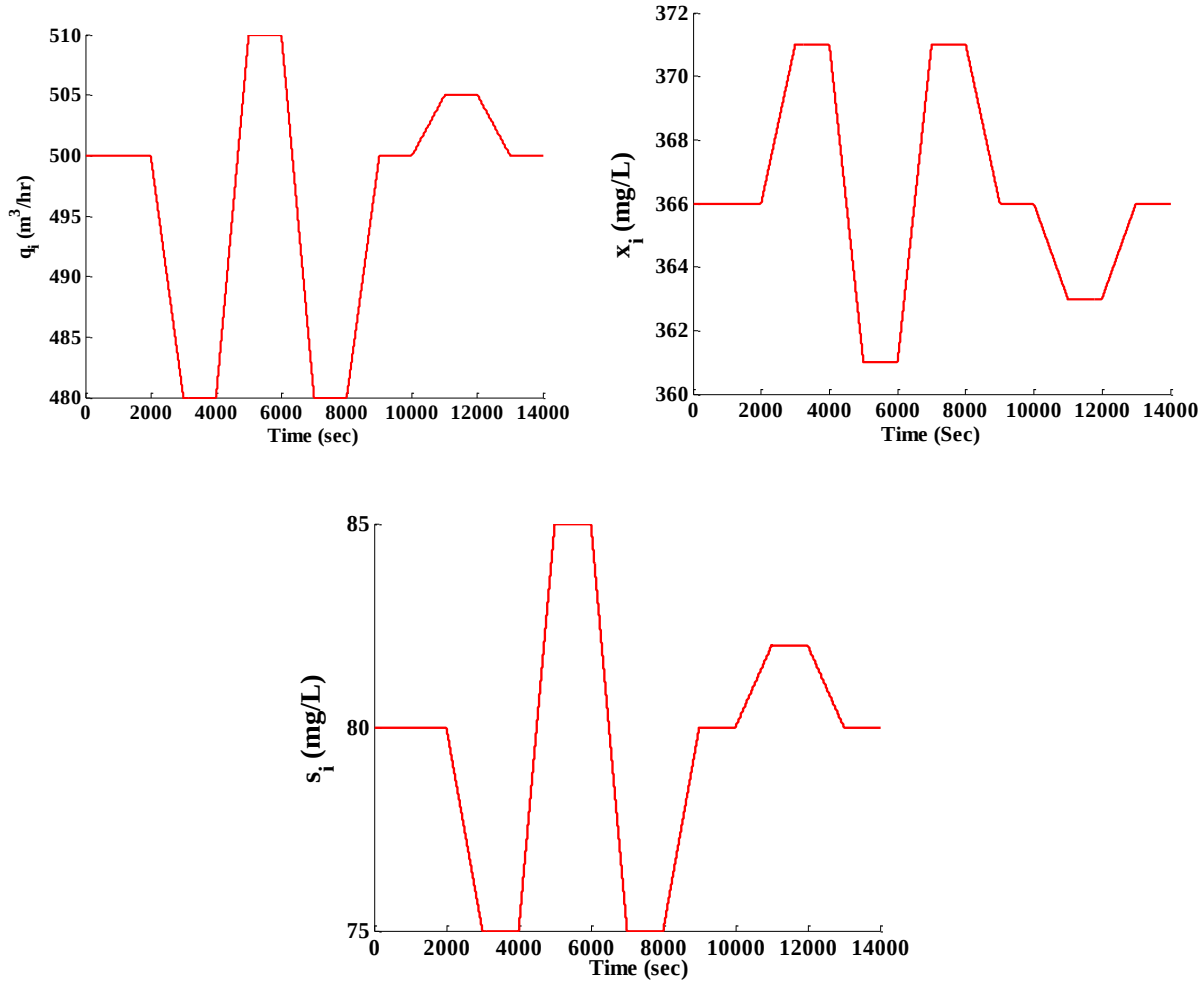

Figure 4.12 Ramp profiles for different Disturbances

The cost function convergence chart obtained for this scenario is shown in Figure 4.13. The results obtained from this scenario are tabulated in Table 4.7 (Scenario 2).

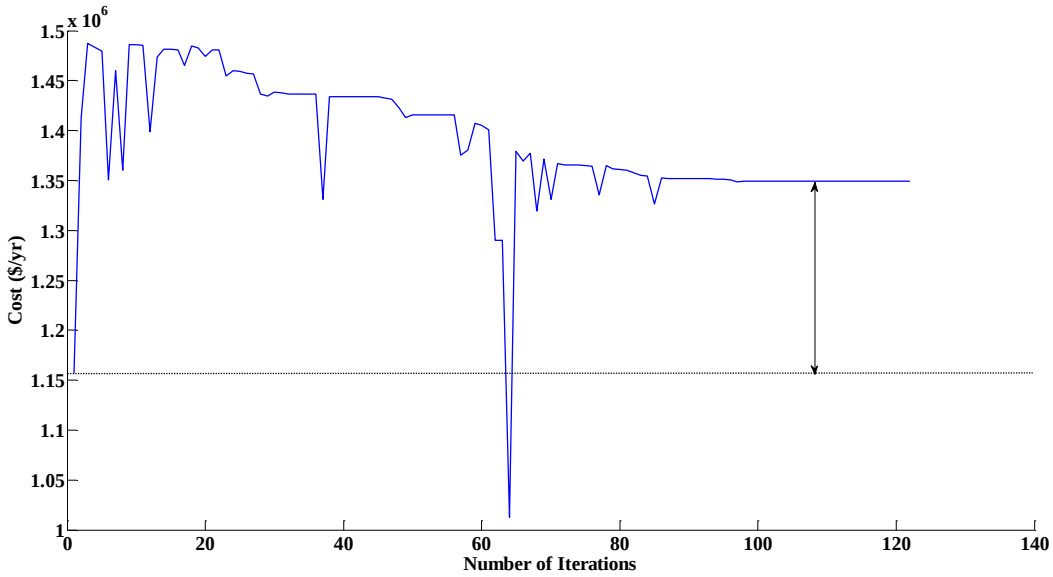

Figure 4.13: Scenario 2: Cost function convergence chart

As shown in Figure 4.13, the optimum cost value was found to be higher by around 15% from the optimal steady state design when ramp changes are used as disturbances. A sudden decrease in the cost at the 62nd iteration is noticed because the sensitivity for the cost function with respect to the area of the decanter (A) changed drastically in that iteration. The cost function converged after 122 iterations when the convergence criteria shown in step 5 of algorithm was used.

As shown in Table 4.7 (Scenario 2), the cost obtained in scenario 2 is around 25% lower than the cost obtained in scenario 1. This is due to the fact that the ramp changes are slow and gradual changes when compared with steps changes where fast dynamics are introduced into the system. It should be noted that the slopes used during the formulation of ramps in the disturbance profile will affect the final cost. The substrate set point s_{sp} converged to a higher value as compared to scenario 1 which in turns reduces the total cost of the system. It should be noted that area (A) and volume (V) also converged to lower values when compared with scenario 1 (See Table 4.7). Figure

4.14 shows the validation for the system when ramps are used to represent the disturbance dynamics. As in scenario 1, the constraint that bounds the substrate concentration is the only active constraint for the present scenario.

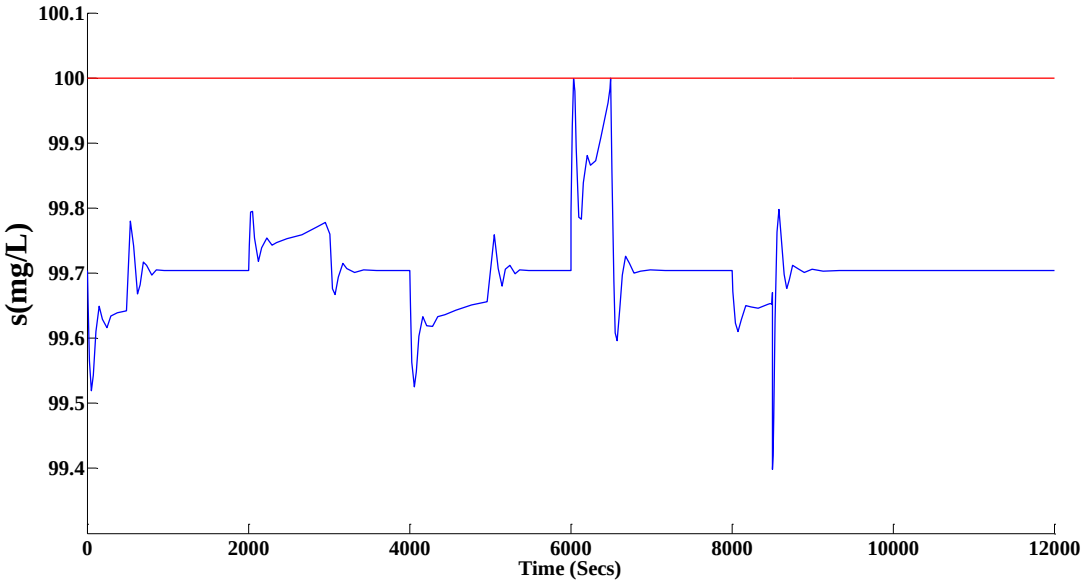

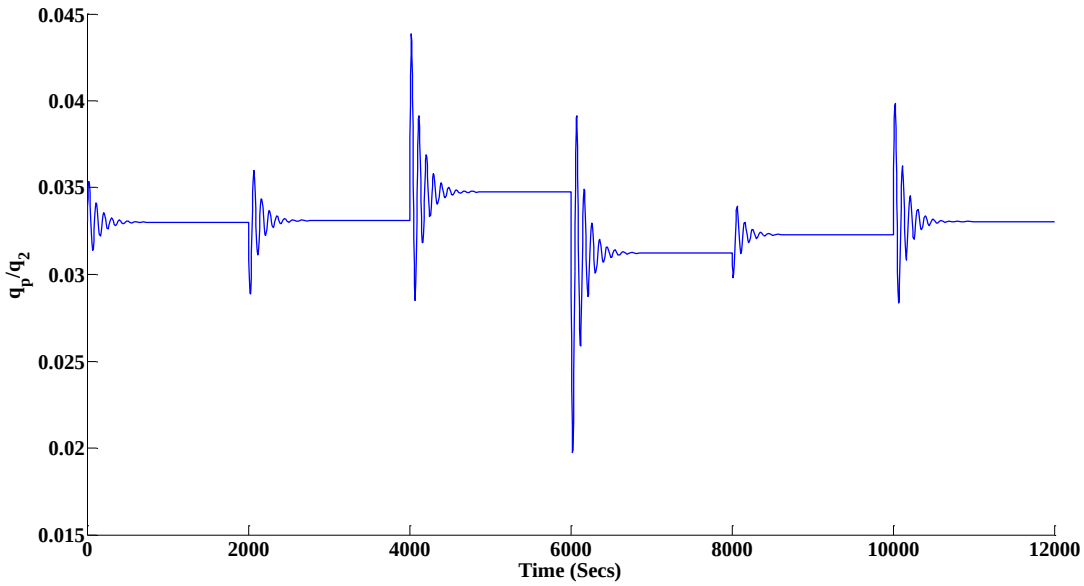

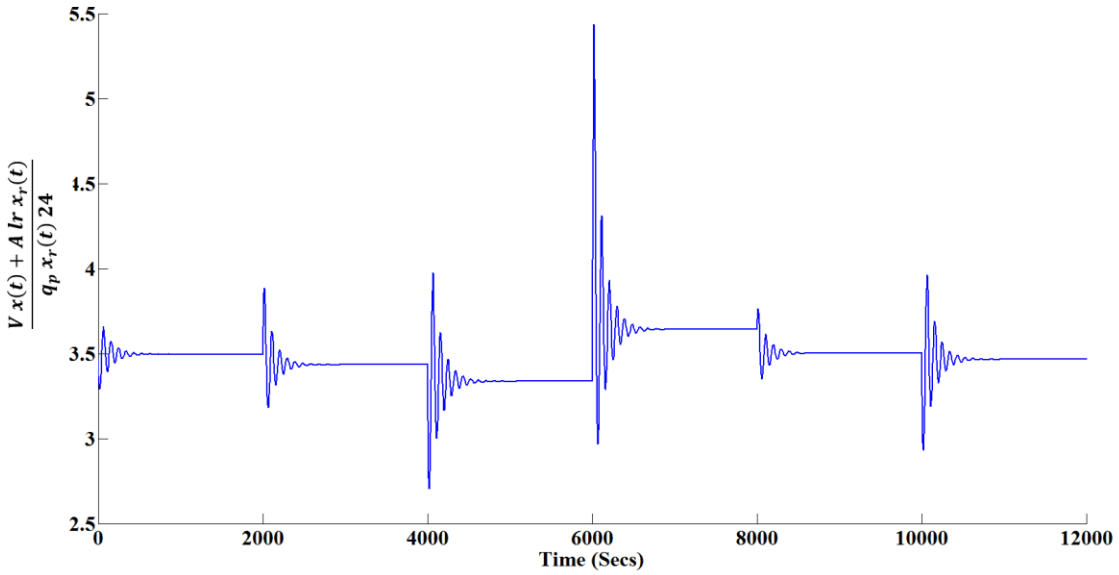

Figure 4.14 Simulating the design: Scenario 2

Scenario 3: Effect of model parameter uncertainty

In the two scenarios discussed above, only the effect of process disturbances was considered. In this scenario, both process disturbances and model parameter uncertainty were taken into consideration. Accordingly, the specific growth rate (μ), biomass death rate (k_d) and the specific cellular activity (k_c) were considered as the uncertain parameters for the present scenario. The uncertain realizations, and their corresponding weights, that were used in the analysis are shown in Table 4.8. Step changes were considered as the disturbance dynamics and they follow the specifications provided for scenario 1, i.e. see equation 4.34.

Table 4.8 Parameter uncertainty descriptions, Waste Water Treatment Plant

specific growth rate (μ),	biomass death rate (k_d)	specific cellular activity (k_c)	Weights (w_j)
0.1824 (h^{-1})	5.00E-05 (h^{-1})	1.33 E-04 (h^{-1})	0.3
1.10*0.1824	1.10*5.00E-05	1.10*1.33 E-04	0.1
0.90*0.1824	0.90* 5.00E-05	0.90*1.33 E-04	0.1
1.10*0.1824	0.90*5.00E-05	1.10*1.33 E-04	0.1
0.90*0.1824	1.10*5.00E-05	0.90*1.33 E-04	0.1
1.05*0.1824	0.95*5.00E-05	1.05*1.33 E-04	0.1
0.95*0.1824	1.10*5.00E-05	0.95*1.33 E-04	0.1
0.98*0.1824	1.07*5.00E-05	0.97*1.33 E-04	0.1

The optimal design and controller tuning parameters obtained for this scenario along with the cost and CPU time are presented in Table 4.7 (Scenario 3). The cost obtained for this scenario is almost 20% higher as compared to Scenario 1 when no uncertainty was introduced. This is due to the fact that multiple realizations in the uncertain parameters were introduced into the system which in turn made the area (A) and the volume (V) to converge to higher values (around 20%) as compared to when no uncertainty was introduced (See Table 4.7). The total CPU time also increases significantly as simulations are needed for each realization in the uncertain parameters. The cost function converged after 62 iterations.

Figure 4.15 shows the validation of the design for this scenario using the process disturbance specification shown in (4.34) and the realizations in the uncertain parameters shown in Table 4.. As shown in this figure, the substrate concentration, the ratio between the purge to the recycle

flow rates and the purge age in the decanter are maintained within their corresponding feasible limits. This demonstrates that the second order PSE approximations employed for the present scenario are valid representations of the actual process constraints and cost function; therefore, dynamic feasibility is guaranteed for the specific disturbances and discrete realizations in the uncertain parameters considered in the analysis. Each line in Figure 4.15 shows the validation for each realization in uncertain parameter (See Table 4.8).

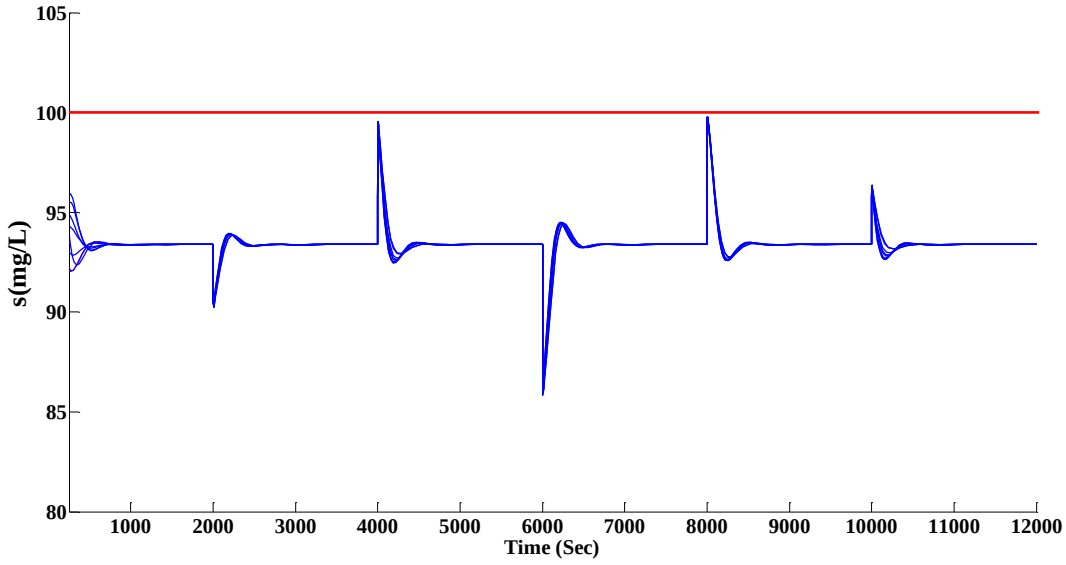

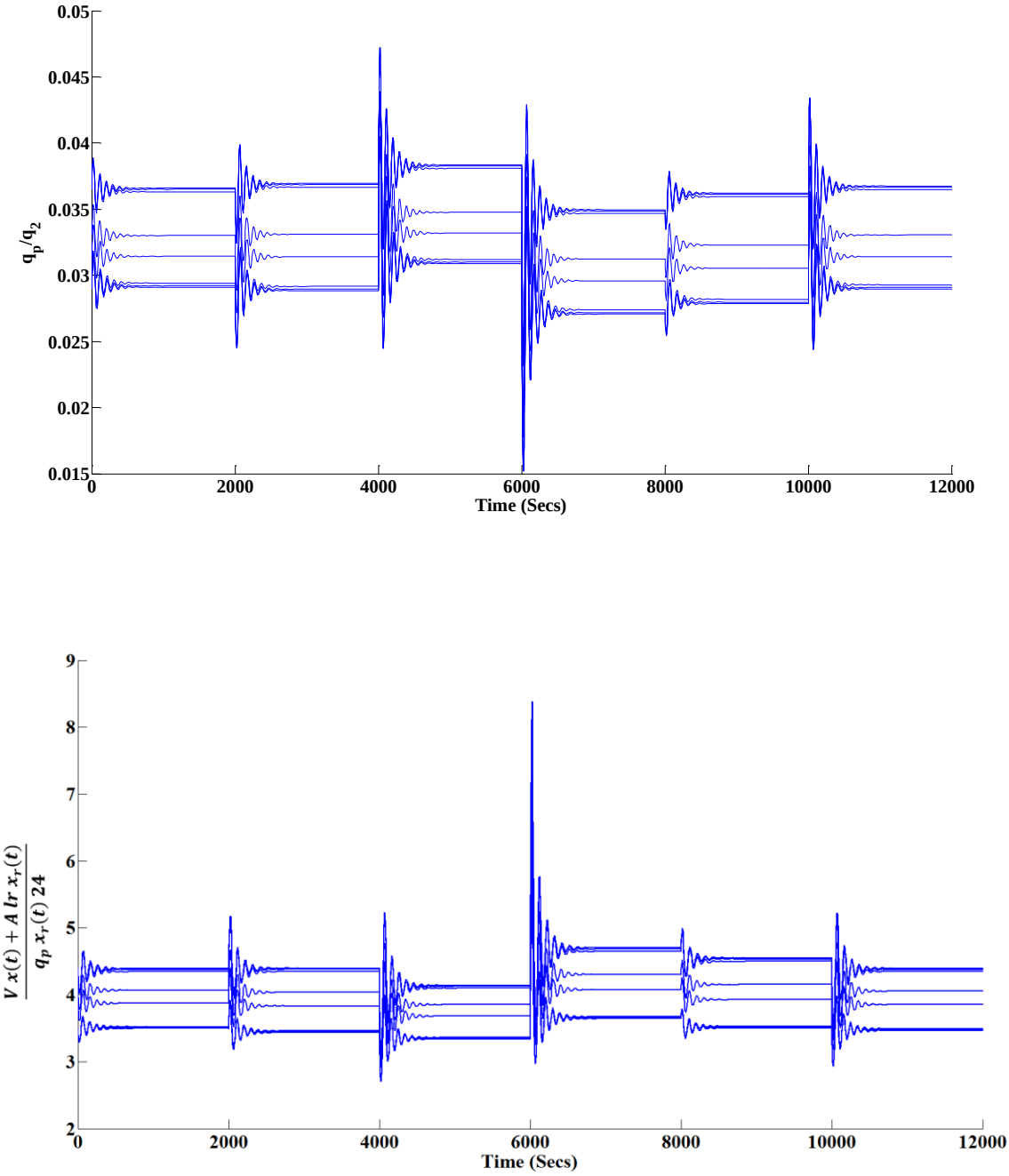

Figure 4.15 Simulating the results: Scenario 3

Summary

This chapter discussed case studies using the PSE-based integration of design and control technique proposed in this work. A non-isothermal CSTR case study has been used in this work to illustrate the benefits and limitations of the present back-off approach. The results show that the present method converges to the optimal solution faster than the formal integration technique; hence, making this methodology a promising computationally attractive algorithm. Effect of tuning parameter δ, which is a key parameter in the present methodology, have been discussed and the results show that quality of the results improves when smaller values of tuning parameter are used at the expense of higher computational costs. The effect of the order of the PSE approximation used in the calculations has also been studied and it shows that the quality in the results is improved when higher orders in the PSE approximations are used at the expense of higher computational costs.

This chapter also presented the implementation of the proposed back-off methodology to a waste water treatment plant. The results from this analysis showed that the system converges to the optimal solution faster than the formal integration technique. The effect of different disturbance dynamics were also studied and the results show the cost is lower when ramps are used as disturbance profile when compared with steps because slow and gradual changes take place in ramp input instead of sudden changes in step inputs. The case of uncertain parameters was also studied and the results showed that a higher cost is obtained when uncertainty is introduced in the system when compared to the scenario where no uncertainty is considered.

Chapter 5

Conclusions and Recommendations

Integration of design and control has emerged as an active area of research as process systems are always subject to external disturbances and parameter uncertainty. Several methodologies have been presented in this field of integration of design and control but no unified framework has been developed. This study uses the idea of back-off from the steady state point to obtain the optimal feasible solution when dynamics and parameter uncertainty considered in the analysis. Power Series Expansions (PSE) approximations are used to represent the cost function and the process constraint with an aim to calculate the optimal design and controller tuning parameters at low computational costs.

5.1 Conclusion

The research work developed in this thesis focuses on developing a new and novel methodology in the field of integration of design and control for chemical processes under process disturbances and parameter uncertainty. The key idea in this methodology is to back-off from the optimal steady state design, which might be infeasible due to process dynamics and parameter uncertainty. The aim is to obtain the optimal design parameters that result in a dynamically feasible and economically attractive process. The challenge in this method is to determine in a systematic fashion the magnitude of the back-off needed to accommodate the transient and feasible operation of the process in presence of disturbances and parameter uncertainty. The work focuses on calculating various optimal design and control parameters by solving various sets of optimization problems in an iterative manner using mathematical expressions obtained

from power series expansions. In this approach, PSE functions are used to obtain analytical expressions of the actual process constraints and are explicitly defined in terms of system's uncertain parameters and the largest variability in a constraint function due to time-varying changes in the disturbances. Also, the PSE approximation for each constraint is developed around a nominal point in the optimization variables and for each realization considered for the uncertain parameters. The PSE-based constraint represents the actual process constraint and can be evaluated faster since it is explicitly defined in the terms of the optimization variables. These approximations are used to determine the direction in the search of optimal design parameters and operating conditions which is required for an economically attractive and dynamically feasible process. Three case studies were considered to demonstrate the performance of the above described methodology. The first case study is an illustrative example of an isothermal storage tank design where the step by step procedure to develop the methodology has been discussed. The second case study is based on the design of a non-isothermal CSTR under process disturbances and parameter uncertainty. This case study shows how the cost function and each of the process constraints are represented using PSE approximations. The results have been discussed in detail and have been also compared with the formal integration technique. The results show the present method converges to the optimal solution faster than the formal integration technique; hence, making this methodology a promising algorithm. Effect of tuning parameter δ, which is a key parameter in the present methodology, have been discussed and the results show that quality of the results improves when smaller values of tuning parameter are used at the expense of higher computational costs. The effect of the order of the PSE approximation used in the calculations has also been studied and it shows that the quality in the results is improved when higher orders in the PSE approximations are used at the expense of

higher computational costs. The case of uncertainty was also studied and the cost obtained for that case study was about four times the cost when no uncertainty was introduced in the system. A third case study featuring the design of a waste water treatment plant was also considered. The waste water treatment plant is a more complex chemical process that involves high degree of nonlinearity. The effect of using disturbance dynamics and parameters uncertainty were considered in the analysis. The results have shown that the present back-off approach is a promising technique to perform integration of design and control.

5.2 Recommendations

The research work presented in this thesis has contributed in the field of integration of design and control. The work can be further extended in several ways which involves working on the assumptions considered during the development of this work as well as taking into account some new factors. Various ways to improve upon the methodology is discussed next.

- *Adaptive formulation for the tuning parameter δ and the order of the PSE approximation*: In the methodology presented in this thesis, the tuning parameter δ and the order of the approximation are chosen off line and are fixed throughout the length of the simulation. One way to improve the quality of the solution is to use an adaptive formulation for the tuning parameter δ and the order of the expansion. These parameters can be updated during the course of the simulation which may result in suitable solutions.

- *Analytical calculation of the gradient*: In the present methodology the gradients have been calculated numerically using the finite difference method. An alternative approach might be to calculate these gradients analytically. Even though this approach may increase the costs, better design solutions may be obtained using the analytical approach.

- *Consider alternative disturbance and parameter uncertainty descriptions*: In this thesis, only steps and ramps were considered as the disturbance dynamics. Different disturbance profiles like oscillatory disturbances can be considered and their effect on the system can be studied. In this research the parameter uncertainty and their corresponding weights are chosen offline. Various sampling techniques like Monte Carlo sampling or the Latin hypercube sampling (LHS) can be used and the effect on the design parameters and the optimal cost can be compared.

Bibliography

[1] Luyben,W.L., "The need for simultaneous design education," in *The integration of process design and control*, Amsterdam, Elsevier, 2004, pp. 10-41.

[2] Seferlis P., Grievink J., "Process design and control structure screening based on economic and static controllability characteristics," *Computers and Chemical Engineering,* vol. 25, pp. 177-188, 2001.

[3] Lenhoff A.M., Morari M., "Design of resilient- processing plants-Process design under consideration of dynamic aspects," *Chemical Engineering Science,* vol. 37, no. 2, pp. 245-258, 1982.

[4] Perkins J.D., Walsh S., "Optimization as a tool for design/ control integrations," *Computers & Chemical Engineering,* vol. 20, pp. 315-323, 1996.

[5] Luyben M.L., Floudas C.A., "Analyzing the interaction of design and control- A multiobjective framework and application to binary distillation synthesis," *Computers & Chemical Engineering,* vol. 18, no. 10, pp. 933-969, 1994.

[6] Alhammadi H.Y., Romagnoli J.A., "Process design and operation incorparting envirnmental,profitability,heat integartion and controllabilty consideration," in *The integartion of process design and control*, Amsterdam, Elsevier B.V., 2004, pp. 264-305.

[7] Mohideen M.L., Perkins J.D., Pistikopolous E.N., "Optimal design of dynamic systems under uncertainty," *AIChE Journal,* vol. 42, no. 8, pp. 2251-2272, 1996.

[8] Bansal V., Perkins J.D. Pistikopolous E.N., "A case study in simultaneous design and control using rigorous, mixed integer dynamic optimization problems," *Industrial & Engineering Chemistry Research,* vol. 41, pp. 760-778, 2002.

[9] Bansal V., Perkins J.D., Pistikopolous, E.N., Ross R.,Van Schijndel J.M.G., "Simultaneous design and control optimization approach," *Computers & Chemical Engineering,* vol. 24, no. 2, pp. 261-266, 2000.

[10] Kookos I.K., "Optimal operation of batch processes under uncertainty: A monte carlo simulation-deterministic optimization approach," *Industrial & Engineering Chemistry Research,* vol. 42, pp. 6815-6820, 2003.

[11] Seferlis P., Grievink J., "Process design and control structure evaluation & screening using non linear sensitivity analysis," in *The integration of process design and control*, Amsterdam, Elsevire B.V., 2004, pp. 326-351.

[12] Chawankul N., Ricardez-Sandoval L.A. ;Budman H., Douglas P.L., "Integration of design and control: A robust control approach using MPC," *The Canadian Journal of Chemical Engineering,* vol. 85, no. 4, pp. 433-446, 2007.

[13] Gerhard J.J., Marquardt W., Monnigmann M., "Normal vectors on critical manifolds for robust design of transient processes in the presence of fast disturbances," *Society for Industrial and Applied Mathematics,* vol. 7, no. 2, pp. 461-490, 2008.

[14] Alvarado-Morales M.; Hamid M.K.A.,Sin G.; Gernaey k.V.; Woodley J.M.; Gani R., "A model based methodology for simultaneous design anc control of a bioethanol production process," *Computers & Chemical Engineering,* vol. 34, pp. 2043-2061, 2010.

[15] Hamid M.K.A,; Sin G.; Gani R., "Integration of process design and controller design for chemical processes using model based methodology.," *Computers & Chemical Engineering,* vol. 34, no. 5, pp. 683-699, 2010.

[16] Mansouri S.S., Sales-Cruz M.; Huusom J.K.; Woodley J.; Gani R., "Integrated process design and control of reactive distillation processes," in *9th IFAC Symposium on Advanced Control of Chemical Processes*, Whistler , Canada, 2015.

[17] Sanchez-Sanchez K.B.,Ricarez-sandoval L.A., "Simultaneous design and control under uncertainty using model predictive controls," *Industrial & Engineering Chemistry Research,* vol. 52, no. 13, pp. 4815-4833, 2013.

[18] Sanchez-Sanchez K.B.; Ricardez-Sandoval L.A., "Simultaneous process synthesis and control design under uncertainty: A worst case performance approach," *AIChE Journal,* vol. 59, no. 7, pp. 2497-2514, 2013.

[19] Bahakim S.S.; Ricardez-Sandoval L.A., "Simultaneous design and MPC-based control for dynamic sytems under uncertainty: A stochastic approach," *Computers & Chemical Engineering,* vol. 63, pp. 66-81, 2014.

[20] Vega P.; Lamanna R.; Revollar S.; Franciso M., "Integrated design and control of chemical processes- Part 2: An illustrative example," *Computers & Chemical Engineering,* vol. 71, pp. 618-635, 2014.

[21] Xia Z.; Zhao J., "Steady state optimization of chemical process with guaranteed robust stability and controllability under parametric uncertainty and disturbances," *Computers & Chemical Engineering,* vol. 77, pp. 116-134, 2015.

[22] Trainor M.; Giannakeas V.; Kiss C.; Ricardez-Sandoval L.A., "Optimal process and control design under uncertainty: A methodology with robust feasibilty and stability analysis," *Chemical Engineering Science,* vol. 104, pp. 1065-1080, 2013.

[23] Ricardez-Sandoval L.A., Budman H.M.; Douglas, P.L., "Integration of design and control for chemical processes: A review of literature and some results," *Annual Reviews in Control,* vol. 33, no. 2, pp. 158-171, 2009.

[24] Yuan Z.; Chen B.; Sin G.; Gani R., "State-of-the-art and progress in the optimization-based simultaneous design and control for chemical processes," *AIChE Journal,* vol. 58, no. 6, pp. 1640-1659, 2012.

[25] Vega P. Lamanna de Rocco R.; Revollar S.; Francisco M., "Integrated design and control of chemical processes -Part 1: revision and classification," *Computers & Chemical Engineering,* vol. 71, pp. 602-617, 2014.

[26] Sakizlis V.Perkins J.D.; Pistikopolous E.N., "Recent advances in optimization based simultaneous process and control design," *Computers & Chemical Engineering,* vol. 28, no. 10, pp. 2069-2086, 2004.

[27] Bahri P.A.; Bandoni J.A.; Romagnoli J.A., "Effect of disturbances in optimizing control : Staedy state open -loop back-off problem," *AIChE Journal,* vol. 42, no. 4, pp. 983-994, 1996.

[28] Bahri P.A.; Bandoni J.A.; Barton G.W.; Romagnoli J.A., "Back -off calculations in optimizing control: A dynamic approach," *Computers & Chemical Engineering,* vol. 19, pp. 699-708, 1995.

[29] Figueroa J.L.,; Bahri P.A.; Bandoni J.A.; Romagnoli J.A., "Economic impact of disturbances and uncertain parameteres in chemical processes- A dynamic back-off analysis," *Computers & Chemical Engineeing,* vol. 20, no. 4, pp. 453-461, 1996.

[30] Kookos I.K.; Perkinds J.D., "An algorithm for simultaneous process and design," *Industrial & Chemical Enginnering Research,* vol. 40, pp. 4079-4083, 2001.

[31] kookos I.K.; Perkins J.D., "The back off approach to simultaneous design and control," in *The integration of process design and control*, Amsterdam, Elsevier B.V., 2004, pp. 216-238.

[32] Bahri P.A., Bandoni J.A.; Romagnoli J.A., "Integrated flexibility and controllabilty analysis in design of chemical processes," *AIChE Journal,* vol. 43, pp. 997-1015, 1997.

[33] Ricardez-Sandoval L.A.; Budman H.M. Douglas P.L., "Simultaneous Design and Control : A new Approach and comaprisions with existing Methodologies," *Industrial & Engineering Chemistry Research,* vol. 49, pp. 2822-2833, 2010.

[34] McKay M.; Beckman R., Conover W., "Comparison of three methods for selecting values of input variables in the analysis of output from a computer code," *Technometrics,* vol. 21, pp. 239-245, 1979.

[35] Florian A., "An efficient sampling scheme: updated latin hypercube sampling," *Probabilistic Engineering Mechanics,* vol. 7, pp. 123-130, 1992.

[36] Hammersley J. Morton K., "A new Monte Carlo technique: antithetic variates," *Mathematical Proceedings of the Cambridge Philosophical Society,* vol. 52, pp. 449-474, 1956.

[37] Freimer M.; Linderoth J.; Thomas D., "The impact of sampling methods on bias and variance in stochastic linear programs," *Computational Optimization and Applications,* vol. 51, pp. 51-75, 2012.

[38] Johnson M.; Moore L.; Ylvisaker D., "Minimax and maximin distance designs," *Journal of Statistical Planning and Inference,* vol. 26, pp. 131-148, 1990.

[39] Kumar D.; Budman H., "Robust nonlinear MPC based on Volterra series and polynomial chaos expansions," *Journal of Process Controls,* vol. 24, no. 1, pp. 304-317, 2014.

[40] Nagy Z.K.; Braatz; R.D., "Distributional uncertainty analysis using power series and polynomial chaos expansions," *Journal of Process Control,* vol. 17, no. 3, pp. 229-240, 2007.

[41] Bahakim S.S.; Rasoulian S.; Ricarez-Sandoval L.A., "Optimal design of large scale chemical processes under uncertainty: A ranking based approach," *AIChE Journal,* vol. 60, no. 9, pp. 3243-3257, 2014.

[42] Bahakim S.S., Ricardez-Sandoval L.A., "Optimal Design of a Post combustion CO2 Capture Pilot-Scale Plant under Process Uncertainty: A Ranking-Based Approach," *Industrial & Engineering Chemistry Research,* vol. 54, no. 15, pp. 3879-3892, 2015.

[43] Rasoulain S.; Ricardez Sandoval L.A., "Robust multivariable estimation and control in an epitaxial thin film growth process under uncertainty," *Journal of Process Control,* vol. 34, pp. 70-81, 2015.

[44] Rasoulian S.;Ricardez Sandoval L.A., "Uncertainty analysis and robust optimization of multiscale process systems with application to epitaxial thin film growth," *Chemical Engineering Science,* vol. 116, pp. 590-600, 2014.

[45] Rasoulain S,; Ricardez-Sandoval L.A., "A robust nonlinear model predictive controller for a multiscale thin film deposition process," *Chemical Engineering Science ,* vol. 136, pp. 38-49, 2015.

[46] Rasoulian S.; Ricardez Sandoval L.A., "Stochastic nonlinear model predictive control applied to a thin film deposition process under uncertainty," *Chemical Engineering Science ,* vol. 140, pp. 90-103, 2016.

[47] Mehta S.; Ricardez Sandoval L.A., "Integration of design and control of dynamic systems under uncertainty," *Industrial & Engineering Chemistry Research ,* vol. 55, no. 2, p. 485–498, 2015.

[48] Feehery W.F.; Tolsma J.E.; Barton P.I., "Efficient sensitivity analysis of large scale differential - algebric systems," *Applied Numerical Mathematics,* vol. 25, pp. 41-54, 1997.

[49] Galan S.; feehery W.F.; Barton P.I., "Parameter senstivity functions for hybrid discrete-continuous systems," *Applied Numerical Mathematics,* vol. 31, pp. 17-47, 1999.

[50] Ricardez-Sandoval L.A.; Douglas .P.L., Budman H.M., "A methodology for the simultaneous design and control of large-scale systems," *Computers & Chemical Engineering,* vol. 35, pp. 307-318, 2011.

[51] Ricardez-Sandoval L.A., "Optimal design and control of dynamic systems under uncertainty: A probablistic Approach," *Computers & Chemical Engineering,* vol. 43, pp. 91-107, 2012.

Appendix (A)

The part of contents of Chapter 3 and 4 has been published in the Industrial Engineering & Chemistry Research Journal [47] .The author of this thesis is the first and main author of this publication and contributed all the technical aspects of the work as well as writing the manuscript.